Supplementary Figure 1

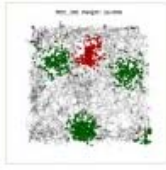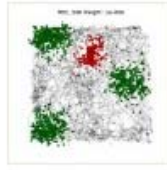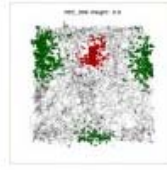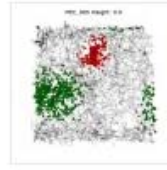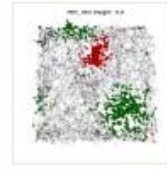|					
input_cell_001.png	input_cell_002.png	input_cell_003.png	input_cell_004.png	input_cell_005.png	input_cell_006.png
input_cell_007.png	input_cell_008.png	input_cell_009.png	input_cell_010.png	input_cell_011.png	input_cell_012.png
input_cell_013.png	input_cell_014.png	input_cell_015.png	input_cell_016.png	input_cell_017.png	input_cell_018.png
input_cell_019.png	input_cell_020.png	input_cell_021.png	input_cell_022.png	input_cell_023.png	input_cell_024.png
input_cell_025.png	input_cell_026.png	input_cell_027.png	input_cell_028.png	input_cell_029.png	input_cell_030.png
input_cell_031.png	input_cell_032.png	input_cell_033.png	input_cell_034.png	input_cell_035.png	input_cell_036.png
input_cell_037.png	input_cell_038.png	input_cell_039.png	input_cell_040.png	input_cell_041.png	input_cell_042.png

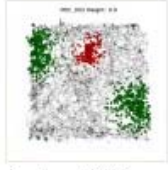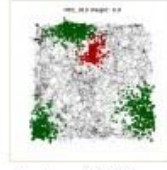input_cell_043.png input_cell_044.png input_cell_045.png input_cell_046.png input_cell_047.png input_cell_048.png
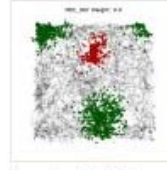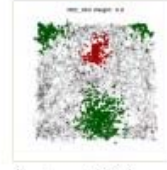
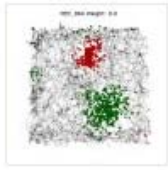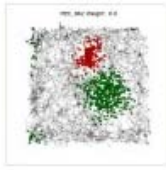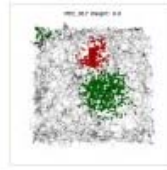input_cell_049.png input_cell_050.png input_cell_051.png input_cell_052.png input_cell_053.png input_cell_054.png
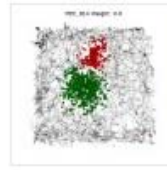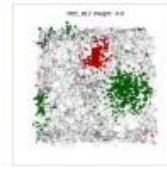
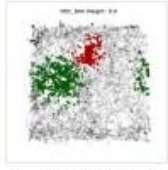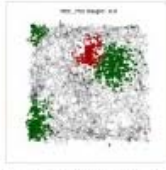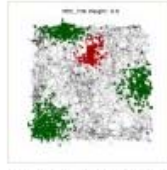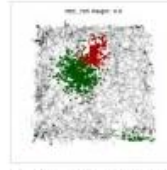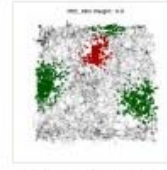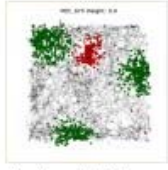input_cell_055.png input_cell_056.png input_cell_057.png input_cell_058.png input_cell_059.png input_cell_060.png
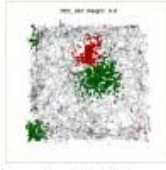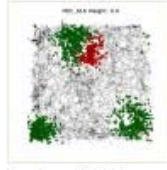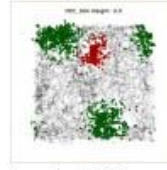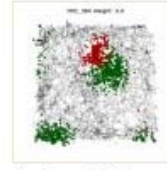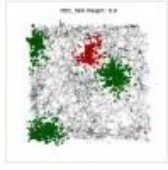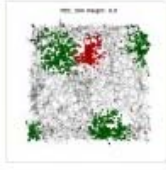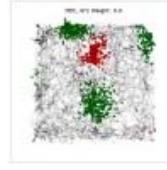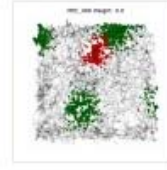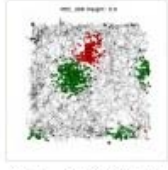
input_cell_061.png input_cell_062.png input_cell_063.png input_cell_064.png input_cell_065.png input_cell_066.png

input_cell_067.png input_cell_068.png input_cell_069.png input_cell_070.png input_cell_071.png input_cell_072.png

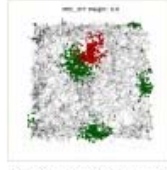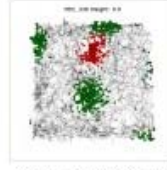input_cell_073.png input_cell_074.png input_cell_075.png input_cell_076.png input_cell_077.png input_cell_078.png
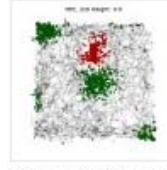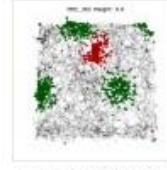
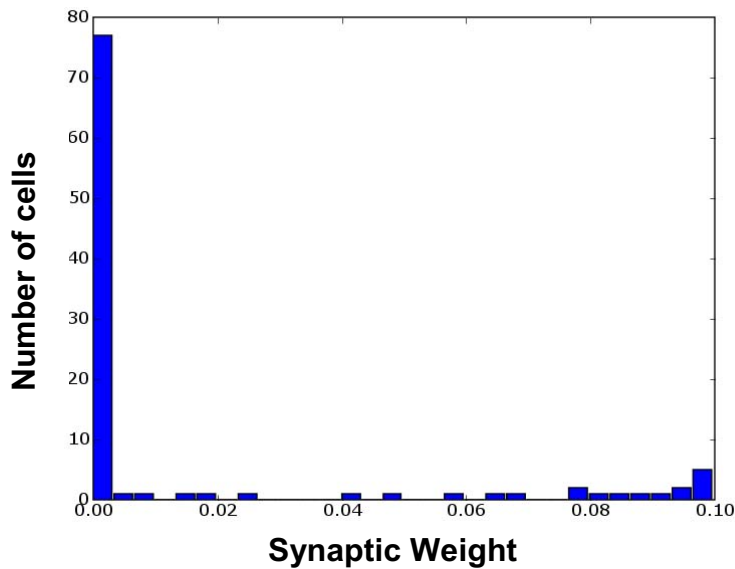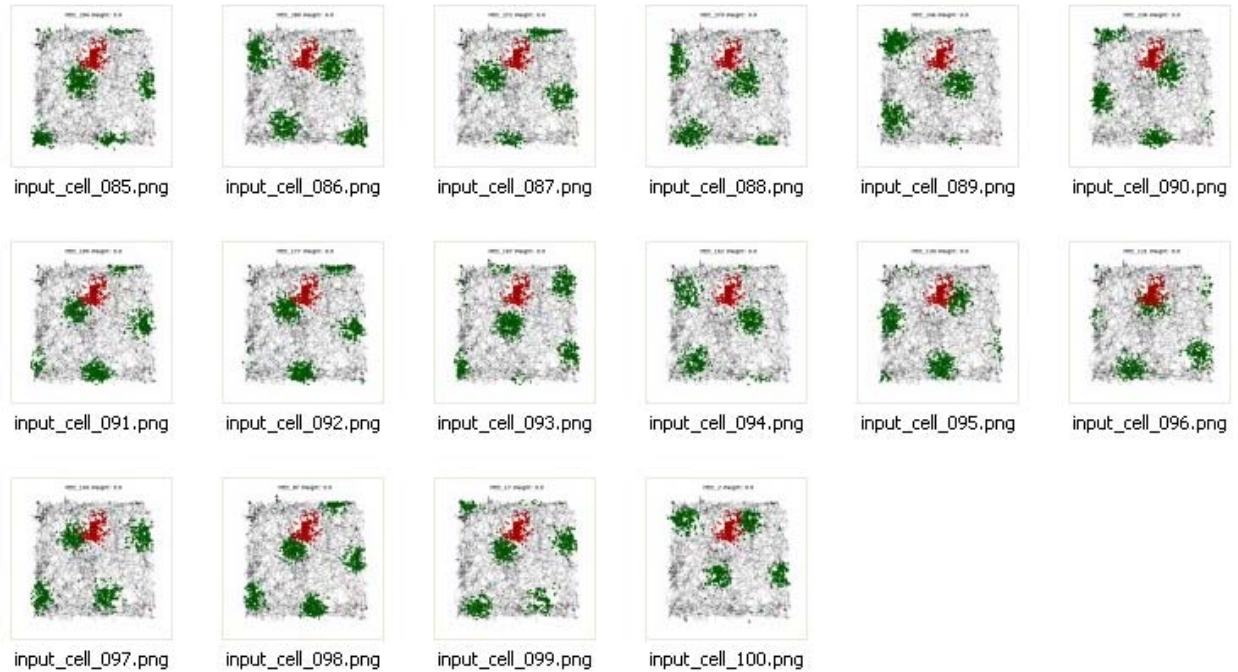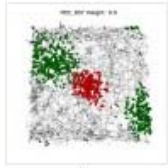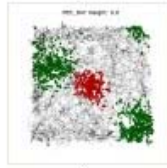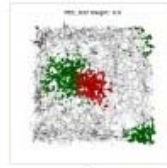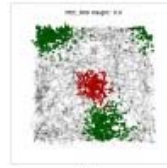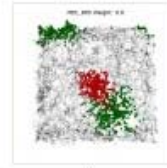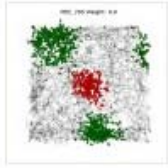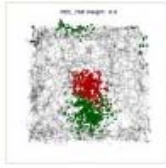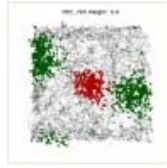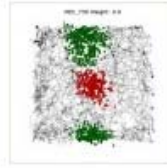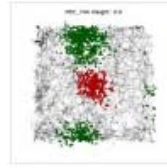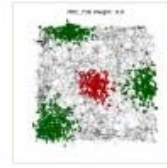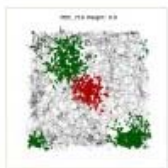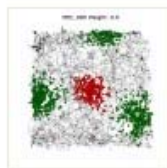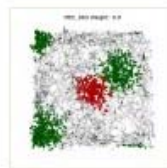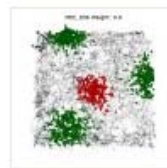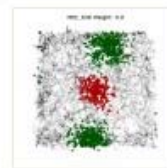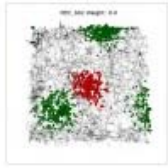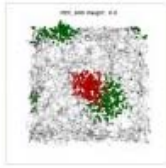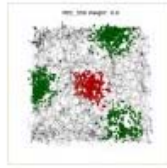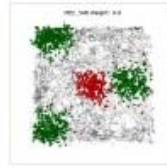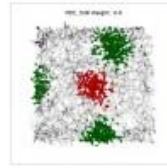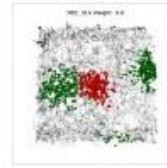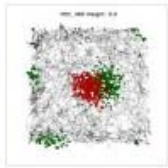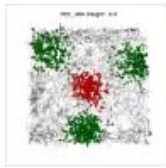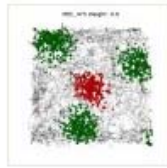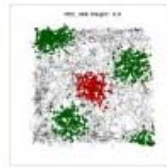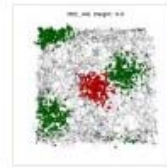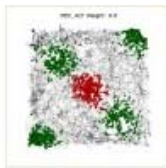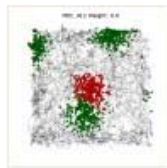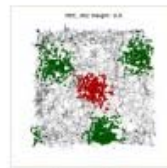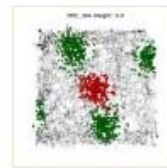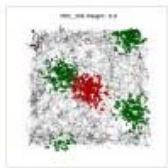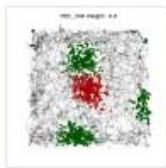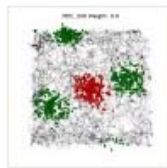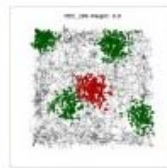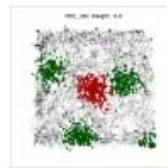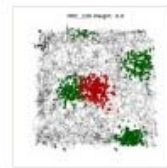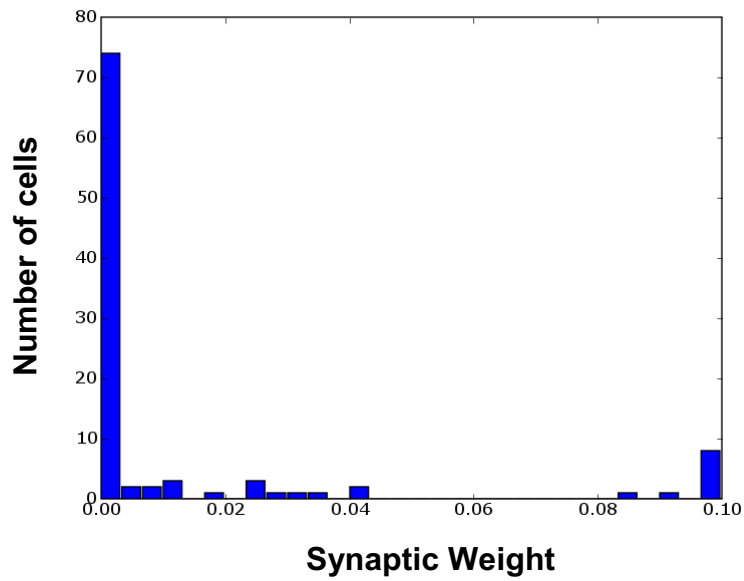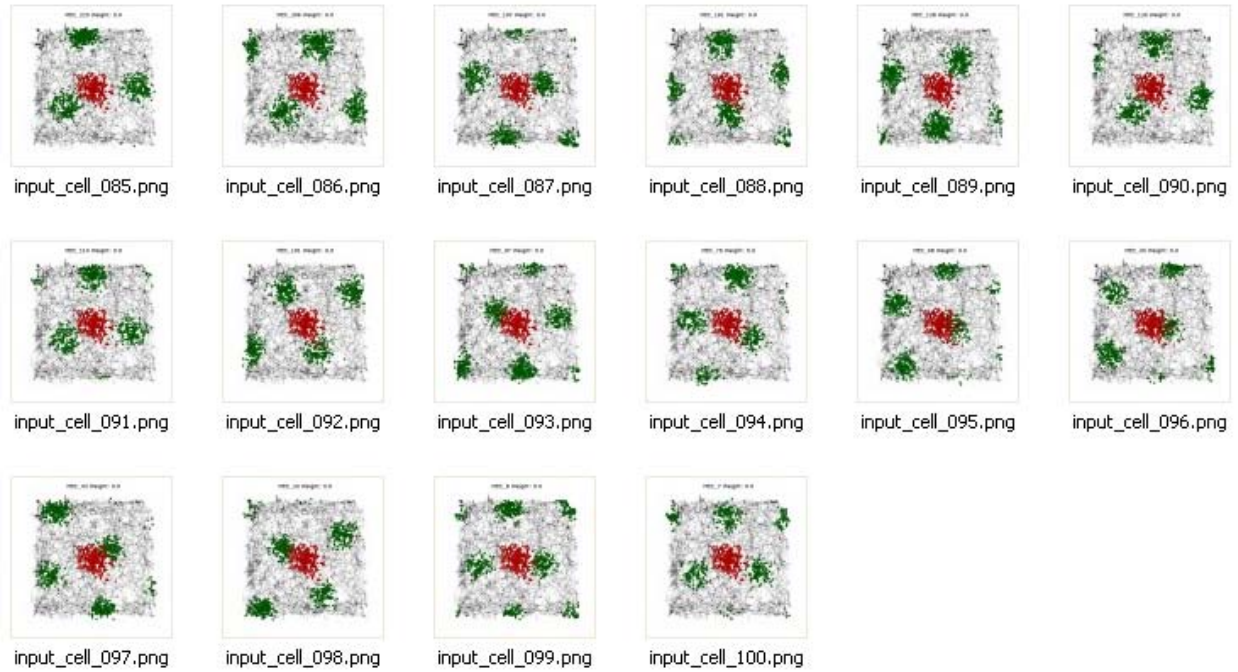input_cell_079.png input_cell_080.png input_cell_081.png input_cell_082.png input_cell_083.png input_cell_084.png
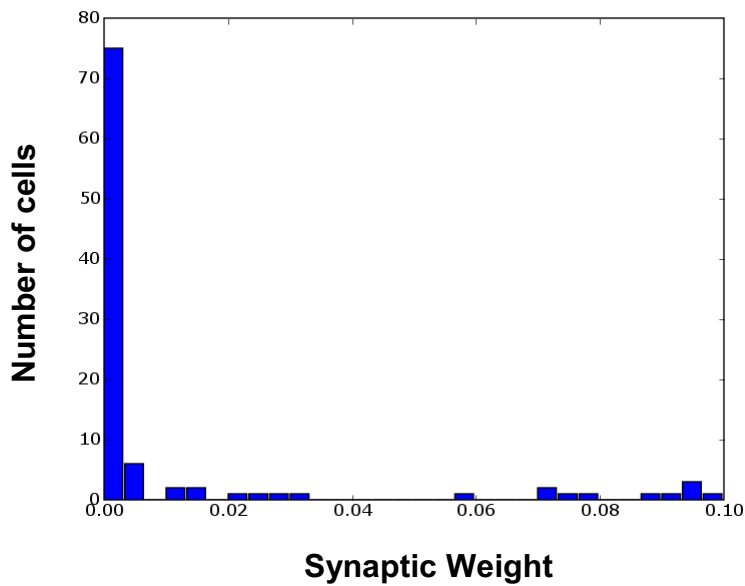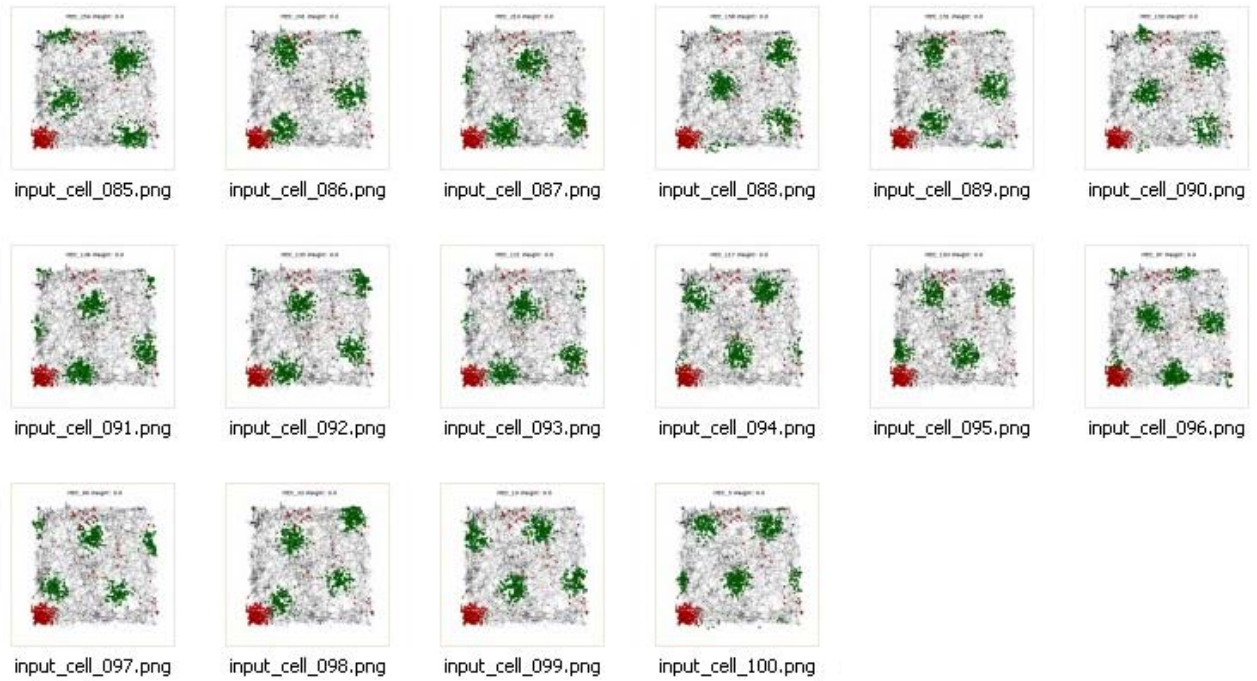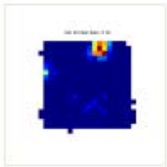
Supplementary Figure 1. Synaptic pattern developed by cell 36 at the end of Simulation 1. This simulation is described in the text and in Figures 2, 3, and 6. (A) Each plot corresponds to one of the 100 grid inputs. The grey line denotes the rat's foraging trajectory over the whole 15-min session (identical across all plots). The green dots denote the locations of the input spikes. The red dots denote the locations of the spikes generated by the output cell (identical across all plots). Grid cells are ordered (from high to low) based on the final strength of the synaptic weight onto the place cell. Inputs that finished the simulation with high weights were those in which one vertex overlapped the place field of the output cell. The remaining inputs, for which the place field typically occurred between vertices, were depressed. (B) The histogram represents the final distribution of synaptic weights ranging from 0 to the saturation limit (0.1 μS).

Supplementary Figure 2

input_cell_001.png input_cell_002.png input_cell_003.png input_cell_004.png input_cell_005.png input_cell_006.png

input_cell_007.png input_cell_008.png input_cell_009.png input_cell_010.png input_cell_011.png input_cell_012.png

input_cell_013.png input_cell_014.png input_cell_015.png input_cell_016.png input_cell_017.png input_cell_018.png

input_cell_019.png input_cell_020.png input_cell_021.png input_cell_022.png input_cell_023.png input_cell_024.png

input_cell_025.png input_cell_026.png input_cell_027.png input_cell_028.png input_cell_029.png input_cell_030.png

input_cell_031.png input_cell_032.png input_cell_033.png input_cell_034.png input_cell_035.png input_cell_036.png

input_cell_037.png input_cell_038.png input_cell_039.png input_cell_040.png input_cell_041.png input_cell_042.png

input_cell_043.png	input_cell_044.png	input_cell_045.png	input_cell_046.png	input_cell_047.png	input_cell_048.png
input_cell_049.png	input_cell_050.png	input_cell_051.png	input_cell_052.png	input_cell_053.png	input_cell_054.png
input_cell_055.png	input_cell_056.png	input_cell_057.png	input_cell_058.png	input_cell_059.png	input_cell_060.png
input_cell_061.png	input_cell_062.png	input_cell_063.png	input_cell_064.png	input_cell_065.png	input_cell_066.png
input_cell_067.png	input_cell_068.png	input_cell_069.png	input_cell_070.png	input_cell_071.png	input_cell_072.png
input_cell_073.png	input_cell_074.png	input_cell_075.png	input_cell_076.png	input_cell_077.png	input_cell_078.png
input_cell_079.png	input_cell_080.png	input_cell_081.png	input_cell_082.png	input_cell_083.png	input_cell_084.png

input_cell_085.png input_cell_086.png input_cell_087.png input_cell_088.png input_cell_089.png input_cell_090.png

input_cell_091.png input_cell_092.png input_cell_093.png input_cell_094.png input_cell_095.png input_cell_096.png

input_cell_097.png input_cell_098.png input_cell_099.png input_cell_100.png

Supplementary Figure 2. Synaptic pattern developed by cell 92 at the end of Simulation 1. (See Supplementary Fig. 1 for legend). These are the same cell and simulation as in Fig. 2.

Supplementary Figure 3

input_cell_001.png   input_cell_002.png   input_cell_003.png   input_cell_004.png   input_cell_005.png   input_cell_006.png

input_cell_007.png   input_cell_008.png   input_cell_009.png   input_cell_010.png   input_cell_011.png   input_cell_012.png

input_cell_013.png   input_cell_014.png   input_cell_015.png   input_cell_016.png   input_cell_017.png   input_cell_018.png

input_cell_019.png   input_cell_020.png   input_cell_021.png   input_cell_022.png   input_cell_023.png   input_cell_024.png

input_cell_025.png   input_cell_026.png   input_cell_027.png   input_cell_028.png   input_cell_029.png   input_cell_030.png

input_cell_031.png   input_cell_032.png   input_cell_033.png   input_cell_034.png   input_cell_035.png   input_cell_036.png

input_cell_037.png   input_cell_038.png   input_cell_039.png   input_cell_040.png   input_cell_041.png   input_cell_042.png

input_cell_043.png   input_cell_044.png   input_cell_045.png   input_cell_046.png   input_cell_047.png   input_cell_048.png

input_cell_049.png   input_cell_050.png   input_cell_051.png   input_cell_052.png   input_cell_053.png   input_cell_054.png

input_cell_055.png   input_cell_056.png   input_cell_057.png   input_cell_058.png   input_cell_059.png   input_cell_060.png

input_cell_061.png   input_cell_062.png   input_cell_063.png   input_cell_064.png   input_cell_065.png   input_cell_066.png

input_cell_067.png   input_cell_068.png   input_cell_069.png   input_cell_070.png   input_cell_071.png   input_cell_072.png

input_cell_073.png   input_cell_074.png   input_cell_075.png   input_cell_076.png   input_cell_077.png   input_cell_078.png

input_cell_079.png   input_cell_080.png   input_cell_081.png   input_cell_082.png   input_cell_083.png   input_cell_084.png

input_cell_085.png   input_cell_086.png   input_cell_087.png   input_cell_088.png   input_cell_089.png   input_cell_090.png

input_cell_091.png   input_cell_092.png   input_cell_093.png   input_cell_094.png   input_cell_095.png   input_cell_096.png

input_cell_097.png   input_cell_098.png   input_cell_099.png   input_cell_100.png

Supplementary Figure 3. Synaptic pattern developed by cell 99 at the end of Simulation 1. (See Supplementary Fig. 1 for legend).

Supplementary Figure 4

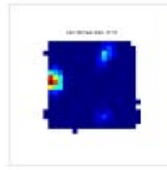|						
CA1_0.png	CA1_1.png	CA1_2.png	CA1_3.png	CA1_4.png	CA1_5.png	CA1_6.png
CA1_7.png	CA1_8.png	CA1_9.png	CA1_10.png	CA1_11.png	CA1_12.png	CA1_13.png
CA1_14.png	CA1_15.png	CA1_16.png	CA1_17.png	CA1_18.png	CA1_19.png	CA1_20.png
CA1_21.png	CA1_22.png	CA1_23.png	CA1_24.png	CA1_25.png	CA1_26.png	CA1_27.png
CA1_28.png	CA1_29.png	CA1_30.png	CA1_31.png	CA1_32.png	CA1_33.png	CA1_34.png
CA1_35.png	CA1_36.png	CA1_37.png	CA1_38.png	CA1_39.png	CA1_40.png	CA1_41.png
CA1_42.png	CA1_43.png	CA1_44.png	CA1_45.png	CA1_46.png	CA1_47.png	CA1_48.png

CA1_49.png   CA1_50.png   CA1_51.png   CA1_52.png   CA1_53.png   CA1_54.png   CA1_55.png

CA1_56.png   CA1_57.png   CA1_58.png   CA1_59.png   CA1_60.png   CA1_61.png   CA1_62.png
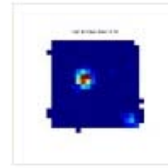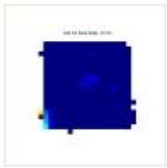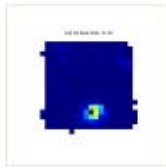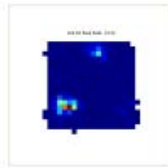
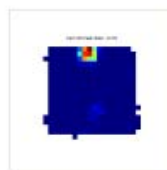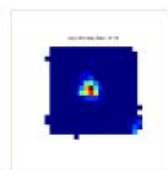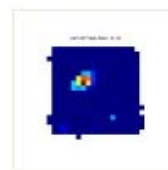CA1_63.png   CA1_64.png   CA1_65.png   CA1_66.png   CA1_67.png   CA1_68.png   CA1_69.png
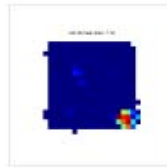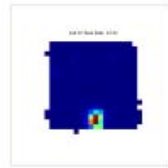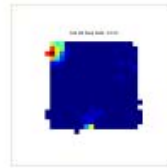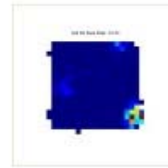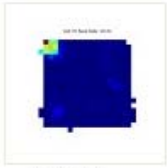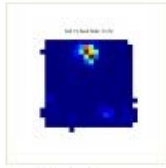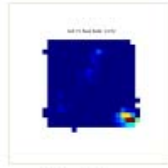
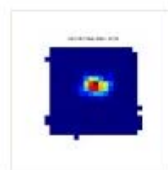CA1_70.png   CA1_71.png   CA1_72.png   CA1_73.png   CA1_74.png   CA1_75.png   CA1_76.png
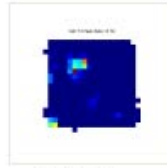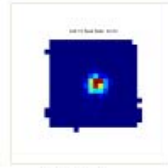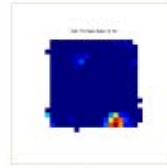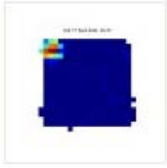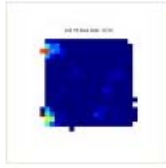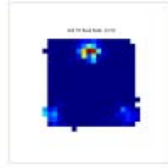
CA1_77.png   CA1_78.png   CA1_79.png   CA1_80.png   CA1_81.png   CA1_82.png   CA1_83.png
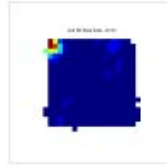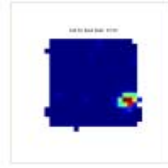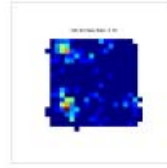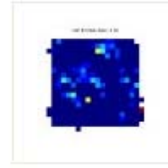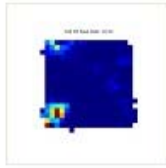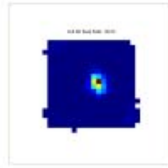
CA1_84.png   CA1_85.png   CA1_86.png   CA1_87.png   CA1_88.png   CA1_89.png   CA1_90.png
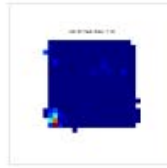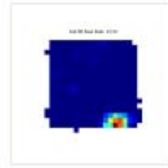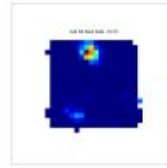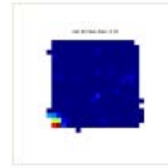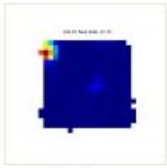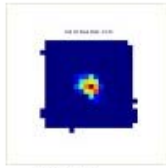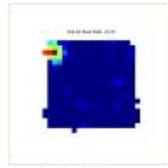
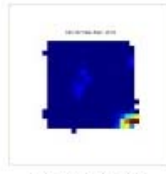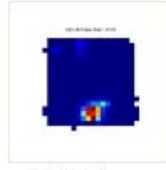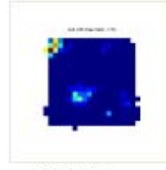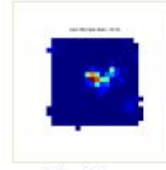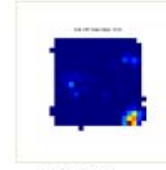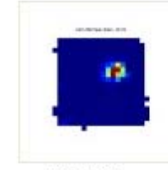CA1_91.png   CA1_92.png   CA1_93.png   CA1_94.png   CA1_95.png   CA1_96.png   CA1_97.png
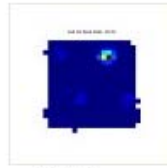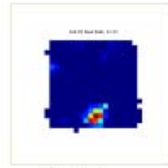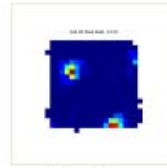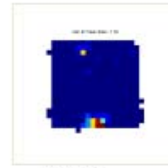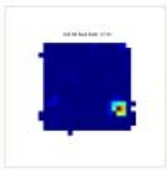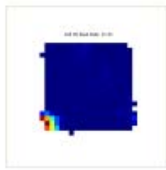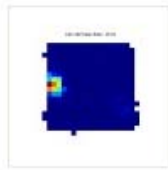
CA1_98.png   CA1_99.png   CA1_100.png   CA1_101.png   CA1_102.png   CA1_103.png   CA1_104.png
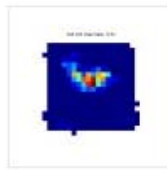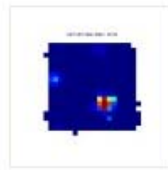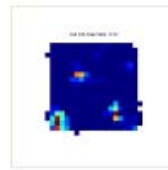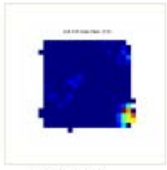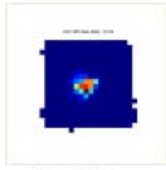
CA1_105.png   CA1_106.png   CA1_107.png   CA1_108.png   CA1_109.png   CA1_110.png   CA1_111.png
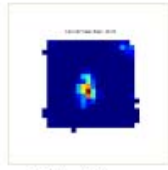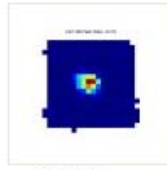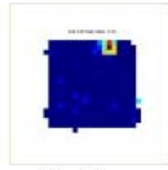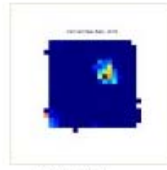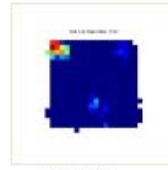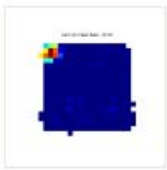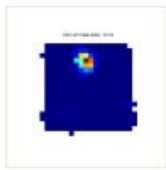
CA1_112.png   CA1_113.png   CA1_114.png   CA1_115.png   CA1_116.png   CA1_117.png   CA1_118.png
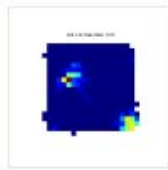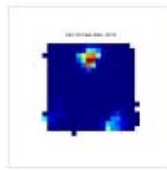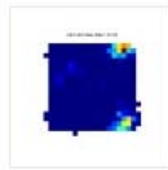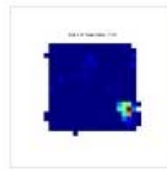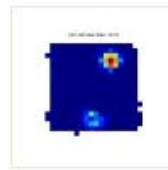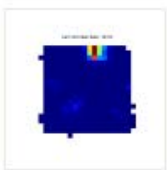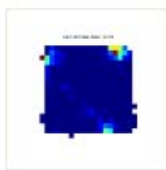
CA1_119.png   CA1_120.png   CA1_121.png   CA1_122.png   CA1_123.png   CA1_124.png   CA1_125.png
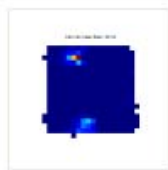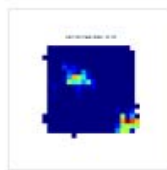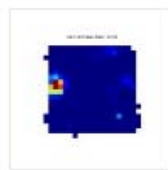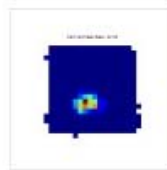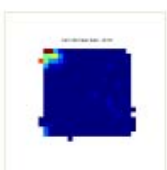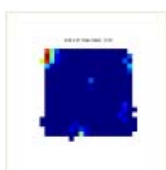
CA1_126.png   CA1_127.png   CA1_128.png   CA1_129.png   CA1_130.png   CA1_131.png   CA1_132.png
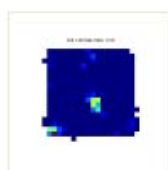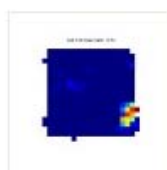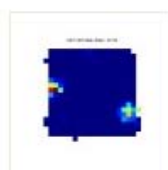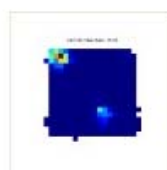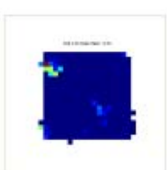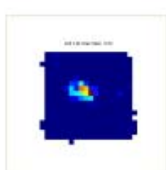
CA1_133.png   CA1_134.png   CA1_135.png   CA1_136.png   CA1_137.png   CA1_138.png   CA1_139.png
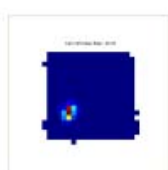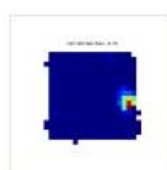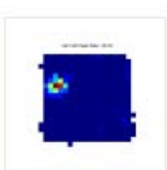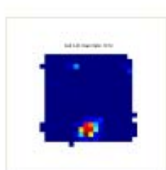
CA1_140.png   CA1_141.png   CA1_142.png   CA1_143.png   CA1_144.png   CA1_145.png   CA1_146.png
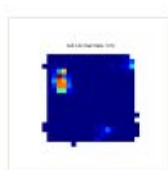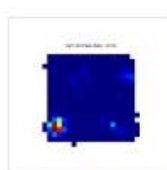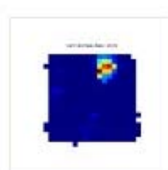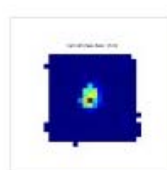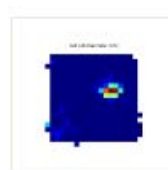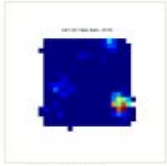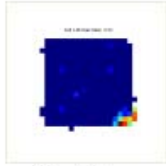
CA1_147.png   CA1_148.png   CA1_149.png   CA1_150.png   CA1_151.png   CA1_152.png   CA1_153.png
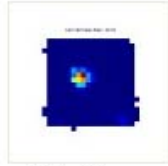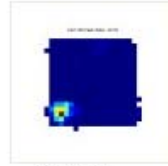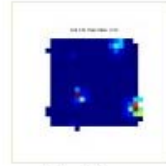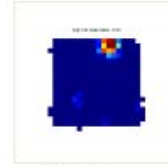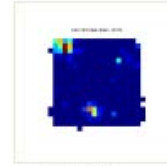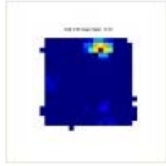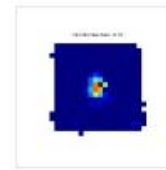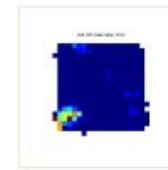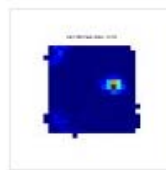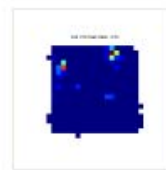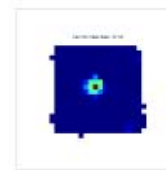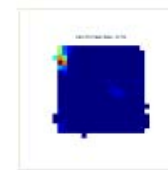
CA1_154.png   CA1_155.png   CA1_156.png   CA1_157.png   CA1_158.png   CA1_159.png   CA1_160.png
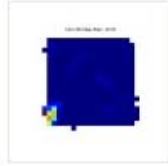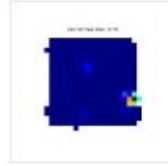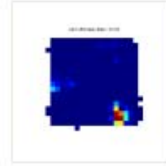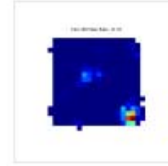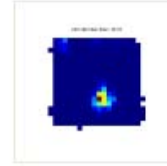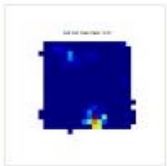
CA1_161.png   CA1_162.png   CA1_163.png   CA1_164.png   CA1_165.png   CA1_166.png   CA1_167.png
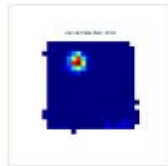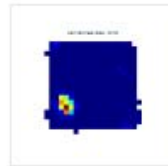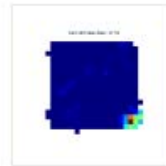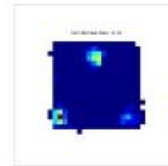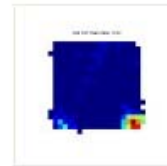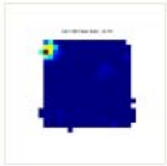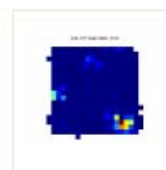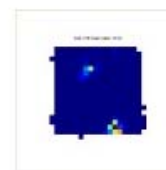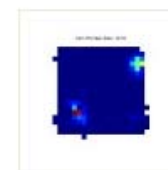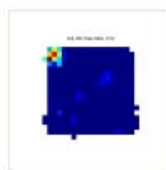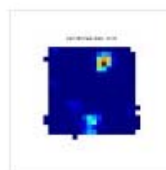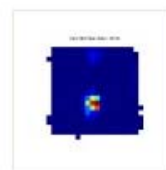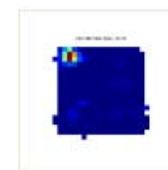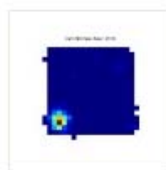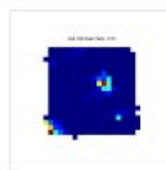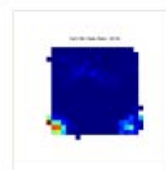
CA1_168.png   CA1_169.png   CA1_170.png   CA1_171.png   CA1_172.png   CA1_173.png   CA1_174.png
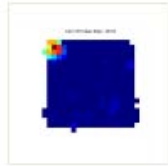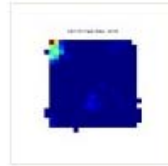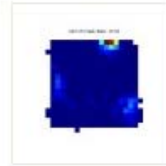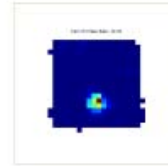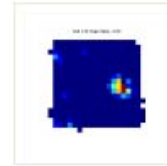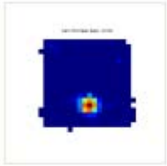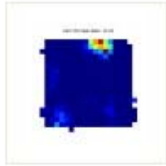
CA1_175.png   CA1_176.png   CA1_177.png   CA1_178.png   CA1_179.png   CA1_180.png   CA1_181.png
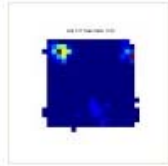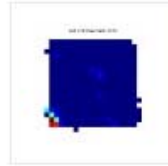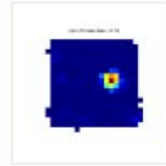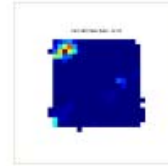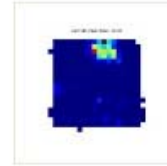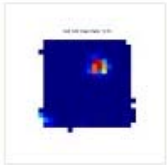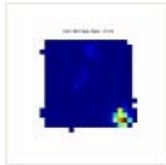
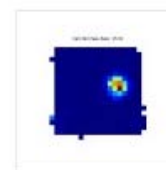CA1_182.png   CA1_183.png   CA1_184.png   CA1_185.png   CA1_186.png   CA1_187.png   CA1_188.png
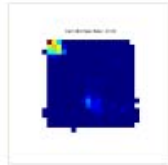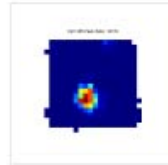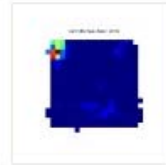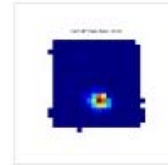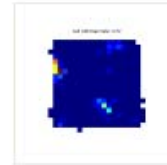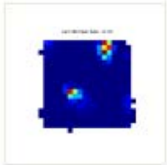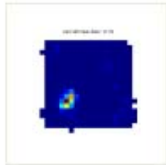
CA1_189.png   CA1_190.png   CA1_191.png   CA1_192.png   CA1_193.png   CA1_194.png   CA1_195.png
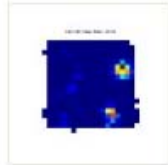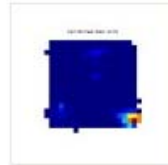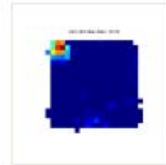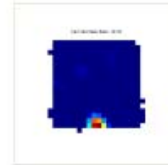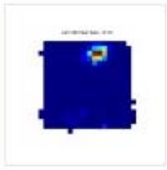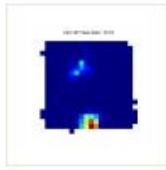
CA1_196.png CA1_197.png CA1_198.png CA1_199.png CA1_200.png CA1_201.png CA1_202.png
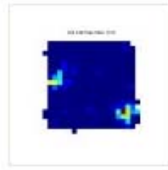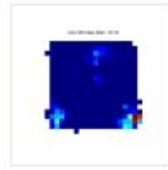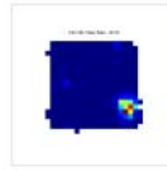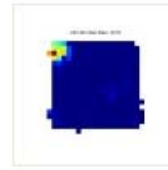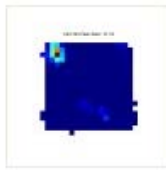
CA1_203.png CA1_204.png CA1_205.png CA1_206.png CA1_207.png CA1_208.png CA1_209.png
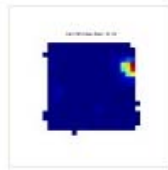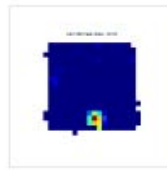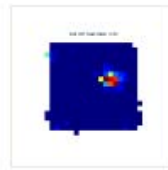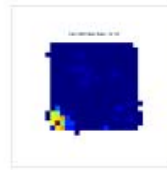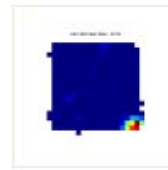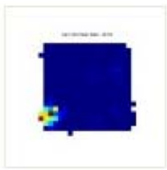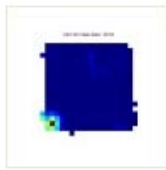
CA1_210.png CA1_211.png CA1_212.png CA1_213.png CA1_214.png CA1_215.png CA1_216.png
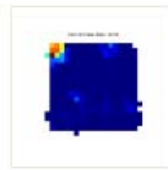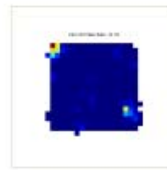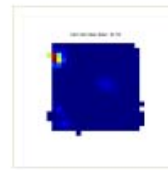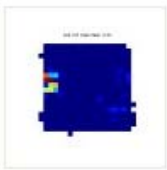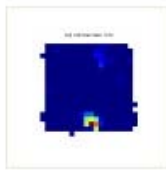
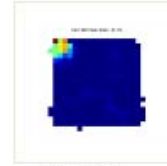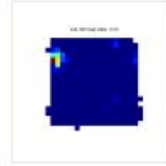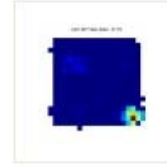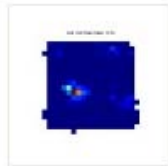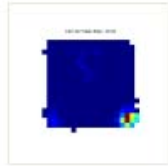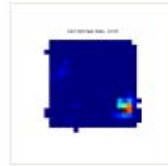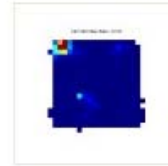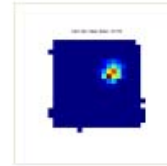CA1_217.png CA1_218.png CA1_219.png CA1_220.png CA1_221.png CA1_222.png CA1_223.png
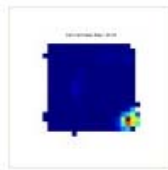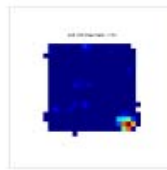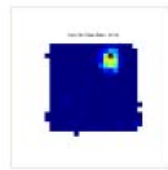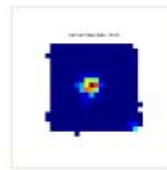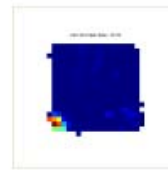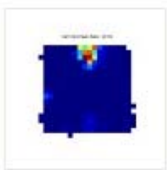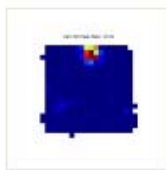
CA1_224.png CA1_225.png CA1_226.png CA1_227.png CA1_228.png CA1_229.png CA1_230.png
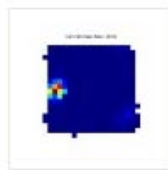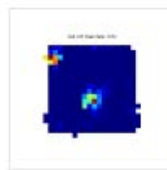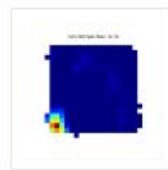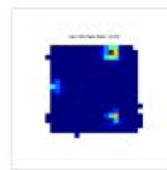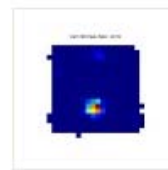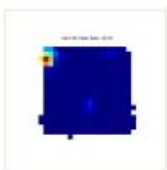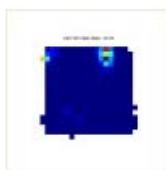
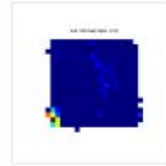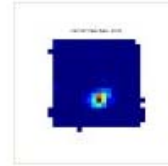CA1_231.png CA1_232.png CA1_233.png CA1_234.png CA1_235.png CA1_236.png CA1_237.png
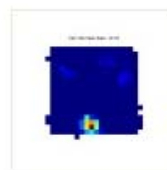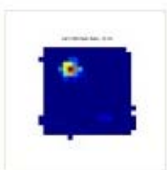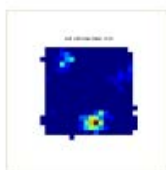
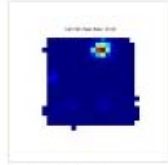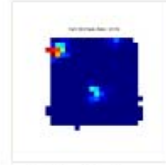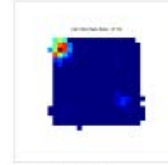CA1_238.png CA1_239.png CA1_240.png CA1_241.png CA1_242.png CA1_243.png CA1_244.png
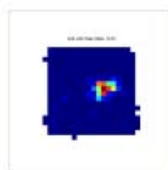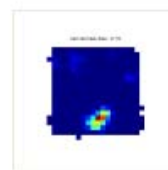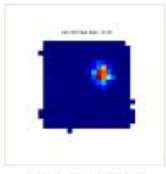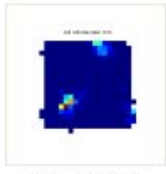
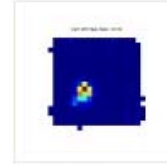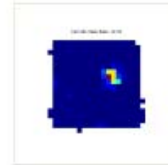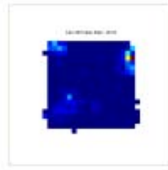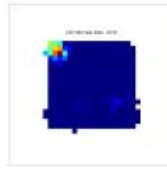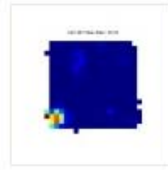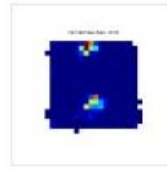CA1_245.png   CA1_246.png   CA1_247.png   CA1_248.png   CA1_249.png   CA1_250.png   CA1_251.png
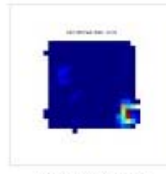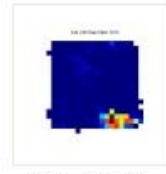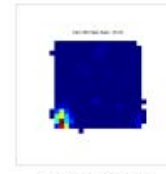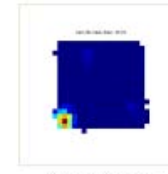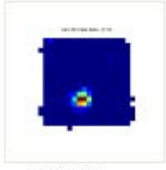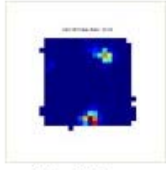
CA1_252.png   CA1_253.png   CA1_254.png   CA1_255.png   CA1_256.png   CA1_257.png   CA1_258.png
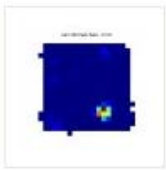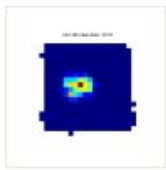
CA1_259.png   CA1_260.png   CA1_261.png   CA1_262.png   CA1_263.png   CA1_264.png   CA1_265.png
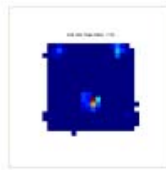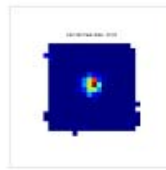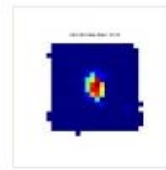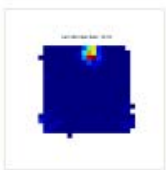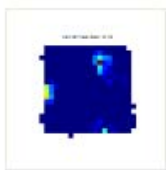
CA1_266.png   CA1_267.png   CA1_268.png   CA1_269.png   CA1_270.png   CA1_271.png   CA1_272.png
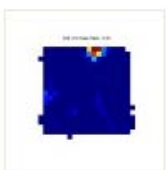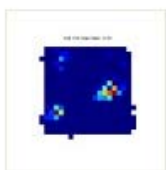
CA1_273.png   CA1_274.png   CA1_275.png   CA1_276.png   CA1_277.png   CA1_278.png   CA1_279.png
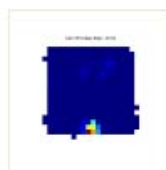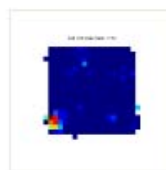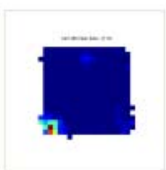
CA1_280.png   CA1_281.png   CA1_282.png   CA1_283.png   CA1_284.png   CA1_285.png   CA1_286.png
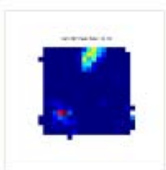
CA1_287.png   CA1_288.png   CA1_289.png   CA1_290.png   CA1_291.png   CA1_292.png   CA1_293.png
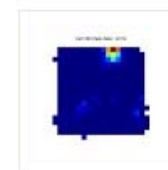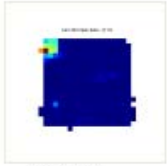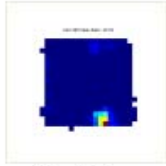
CA1_294.png CA1_295.png CA1_296.png CA1_297.png CA1_298.png CA1_299.png CA1_300.png
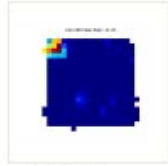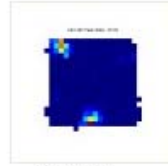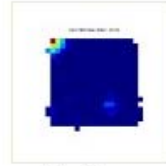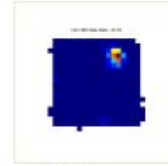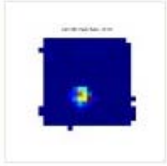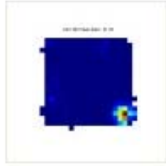
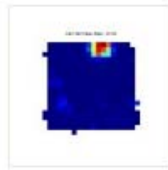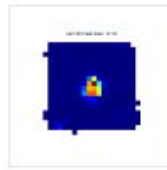CA1_301.png CA1_302.png CA1_303.png CA1_304.png CA1_305.png CA1_306.png CA1_307.png
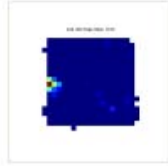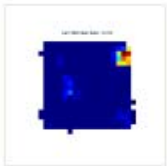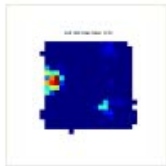
CA1_308.png CA1_309.png CA1_310.png CA1_311.png CA1_312.png CA1_313.png CA1_314.png
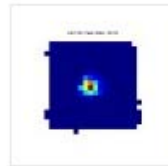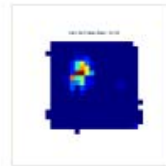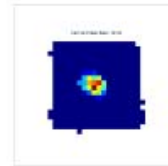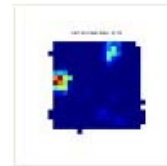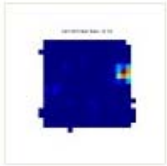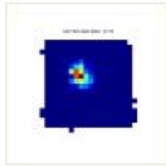
CA1_315.png CA1_316.png CA1_317.png CA1_318.png CA1_319.png CA1_320.png CA1_321.png
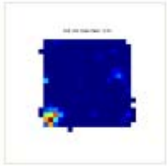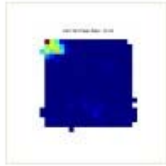
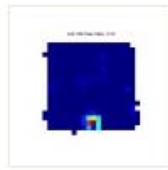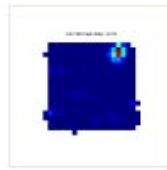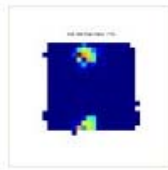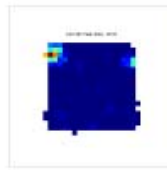CA1_322.png CA1_323.png CA1_324.png CA1_325.png CA1_326.png CA1_327.png CA1_328.png
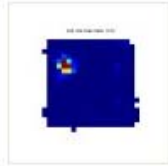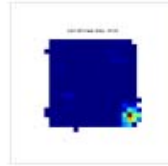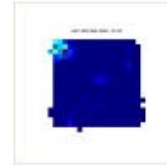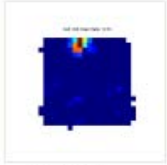
CA1_329.png CA1_330.png CA1_331.png CA1_332.png CA1_333.png CA1_334.png CA1_335.png
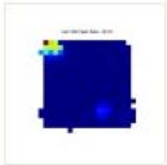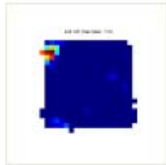
CA1_336.png CA1_337.png CA1_338.png CA1_339.png CA1_340.png CA1_341.png CA1_342.png
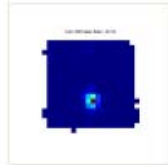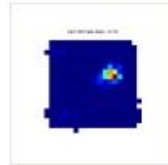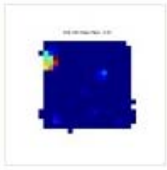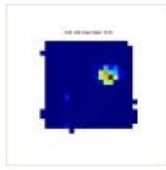
CA1_343.png   CA1_344.png   CA1_345.png   CA1_346.png   CA1_347.png   CA1_348.png   CA1_349.png
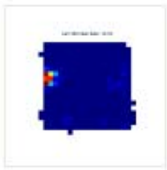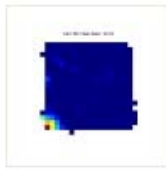
CA1_350.png   CA1_351.png   CA1_352.png   CA1_353.png   CA1_354.png   CA1_355.png   CA1_356.png
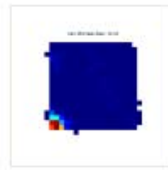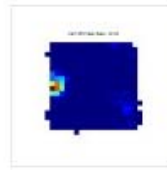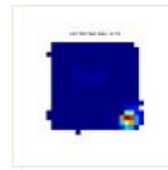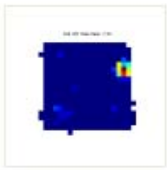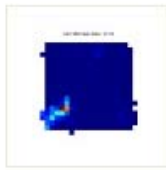
CA1_357.png   CA1_358.png   CA1_359.png   CA1_360.png   CA1_361.png   CA1_362.png   CA1_363.png
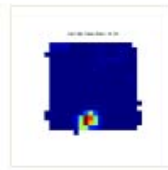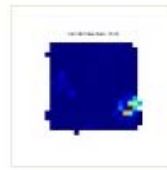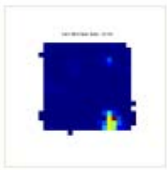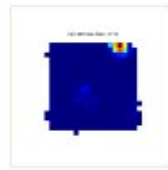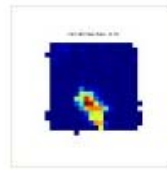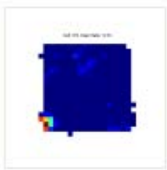
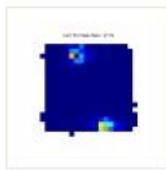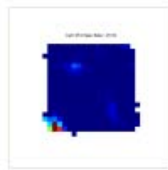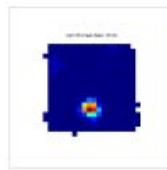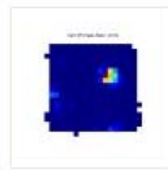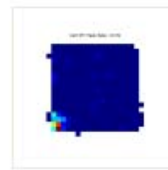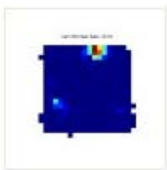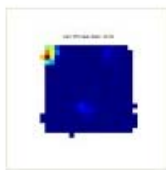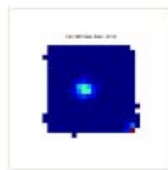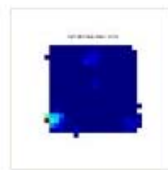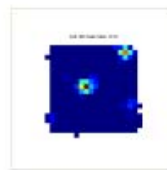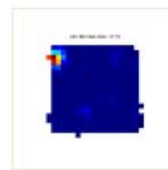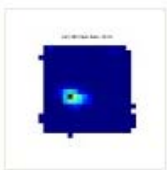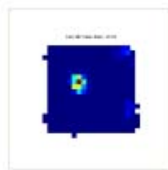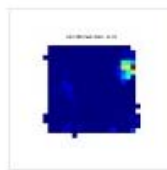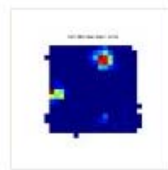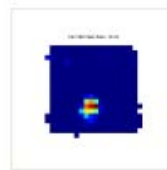CA1_364.png   CA1_365.png   CA1_366.png   CA1_367.png   CA1_368.png   CA1_369.png   CA1_370.png

CA1_371.png   CA1_372.png   CA1_373.png   CA1_374.png   CA1_375.png   CA1_376.png   CA1_377.png

CA1_378.png   CA1_379.png   CA1_380.png   CA1_381.png   CA1_382.png   CA1_383.png   CA1_384.png
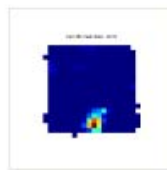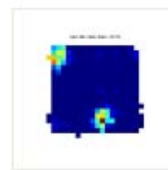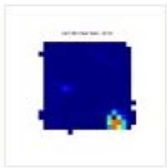
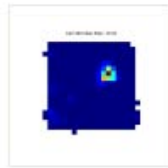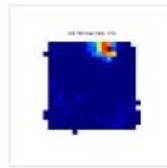CA1_385.png   CA1_386.png   CA1_387.png   CA1_388.png   CA1_389.png   CA1_390.png   CA1_391.png
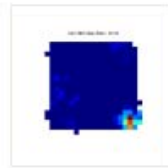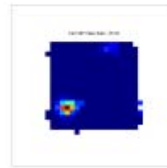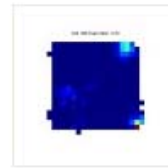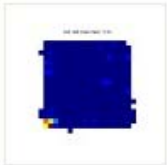
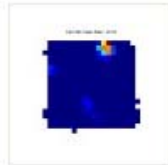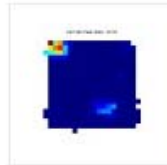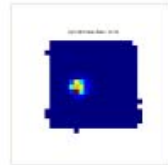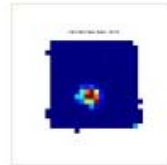CA1_392.png CA1_393.png CA1_394.png CA1_395.png CA1_396.png CA1_397.png CA1_398.png
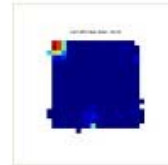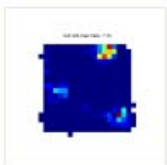
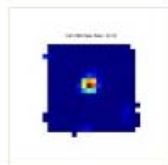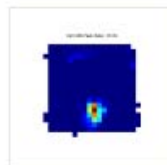CA1_399.png CA1_400.png CA1_401.png CA1_402.png CA1_403.png CA1_404.png CA1_405.png
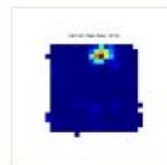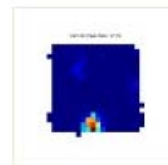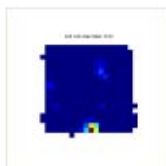
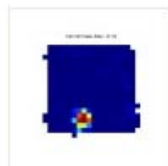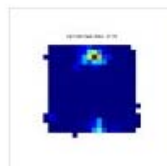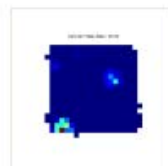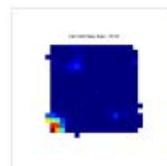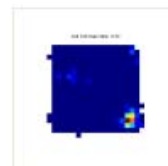CA1_406.png CA1_407.png CA1_408.png CA1_409.png CA1_410.png CA1_411.png CA1_412.png
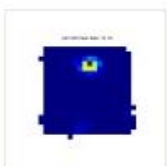
CA1_413.png CA1_414.png CA1_415.png CA1_416.png CA1_417.png CA1_418.png CA1_419.png
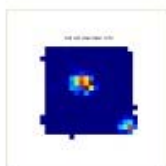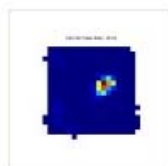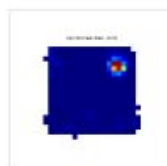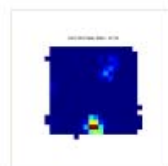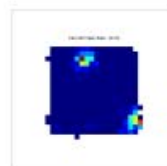
CA1_420.png CA1_421.png CA1_422.png CA1_423.png CA1_424.png CA1_425.png CA1_426.png
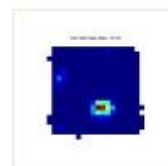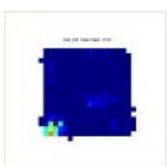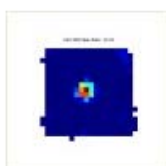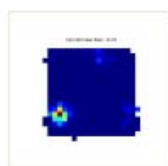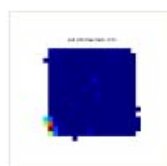
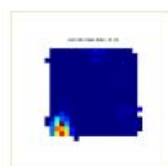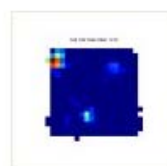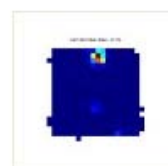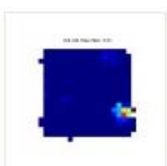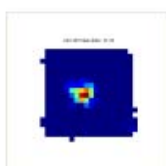CA1_427.png CA1_428.png CA1_429.png CA1_430.png CA1_431.png CA1_432.png CA1_433.png
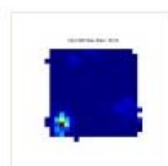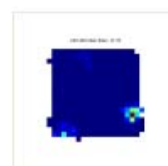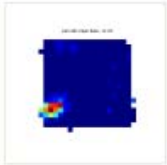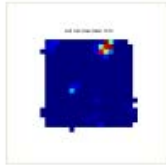
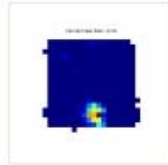CA1_434.png CA1_435.png CA1_436.png CA1_437.png CA1_438.png CA1_439.png CA1_440.png

CA1_441.png

CA1_442.png

CA1_443.png
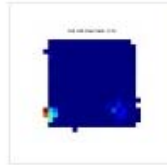
CA1_444.png

CA1_445.png

CA1_446.png

CA1_447.png

CA1_448.png

CA1_449.png

CA1_450.png

CA1_451.png

CA1_452.png

CA1_453.png

CA1_454.png

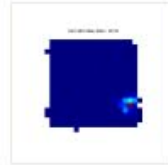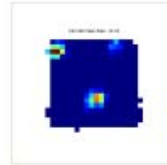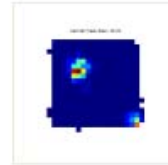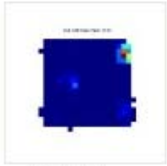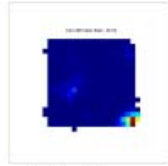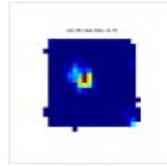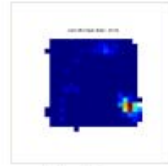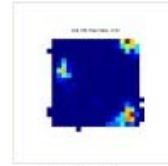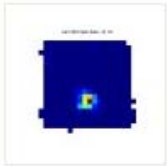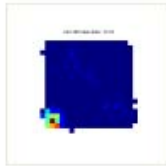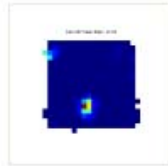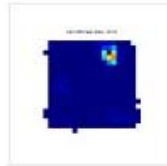CA1_455.png

CA1_456.png

CA1_457.png

CA1_458.png
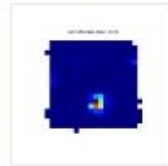
CA1_459.png

CA1_460.png

CA1_461.png

CA1_462.png

CA1_463.png

CA1_464.png

CA1_465.png

CA1_466.png

CA1_467.png

CA1_468.png

CA1_469.png

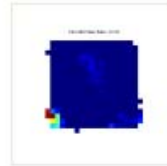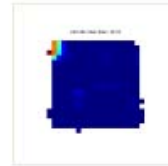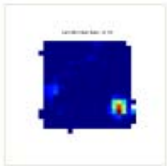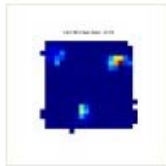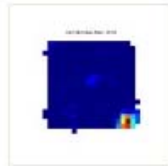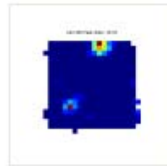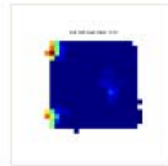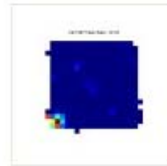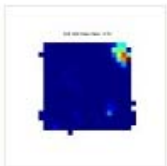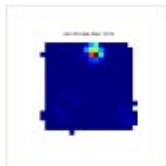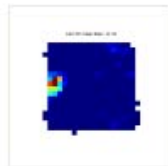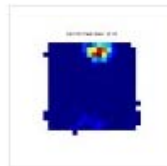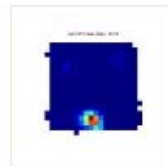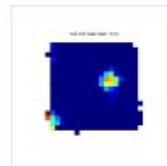CA1_470.png

CA1_471.png

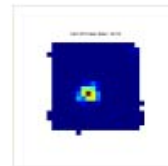
CA1_472.png

CA1_473.png

CA1_474.png

CA1_475.png
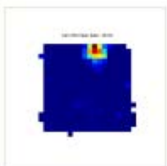
CA1_476.png

CA1_477.png
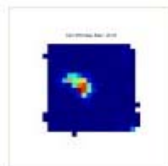
CA1_478.png

CA1_479.png

CA1_480.png

CA1_481.png

CA1_482.png

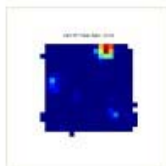
CA1_483.png

CA1_484.png

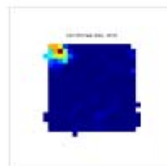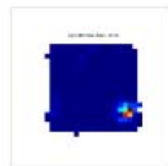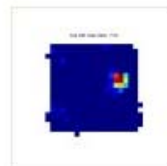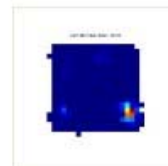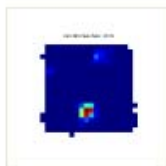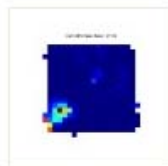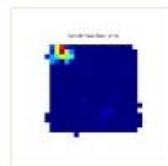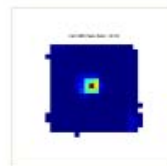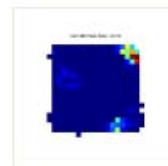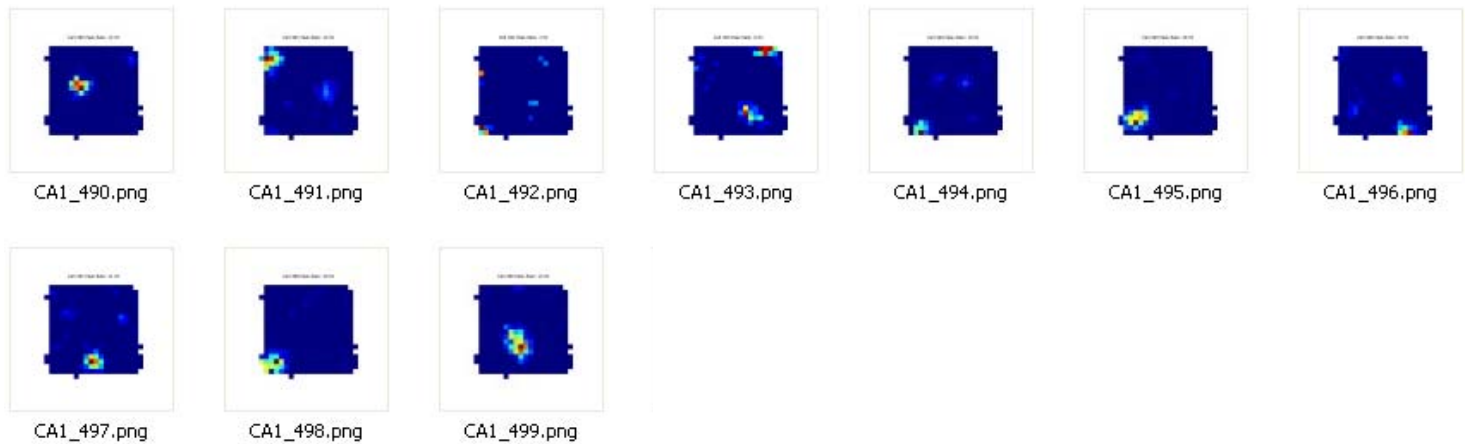
CA1_485.png

CA1_486.png

CA1_487.png

CA1_488.png

CA1_489.png

Supplementary Figure 4. Firing rate maps of all the 'place cells' simulated in Simulation 1. The cells are ordered based on the original numbering of the output cells in the simulation. Spatial information scores (Skaggs et al., 1996) were calculated from the rate maps and were compared with the scores of place field maps produced by random shuffling of the spike train with the position data for each cell (a standard statistical analysis for place-field data). In all cases, the information score for the original rate map was greater than the scores produced by 100 random shuffles. It is possible that this result could be obtained if a cell fired a single burst of spikes at one location. However, the place-field definition criterion of > 0.033 Hz firing rate meant that the cell had to fire a minimum of 30 spikes in the 15-min session to meet criterion as a place field. In fact, in Simulation 1, 497/500 cells produced at least 50 spikes, and 484/500 cells produced at least 100 spikes. Visual inspection of the session data showed that all cells fired at multiple time points in the session. Thus, the significant p values for spatial information for all 500 cells show that all output cells in this simulation provided a reliable spatial signal that was not an artifact of one or two random bursts of activity.
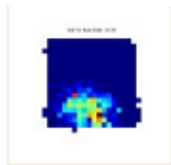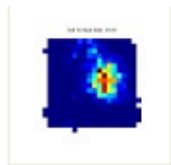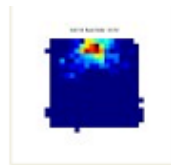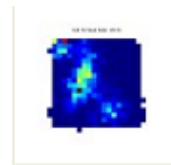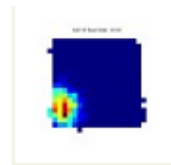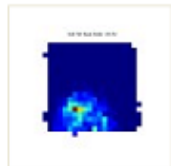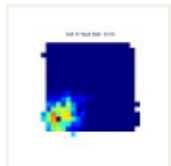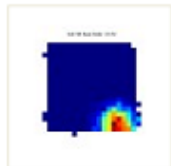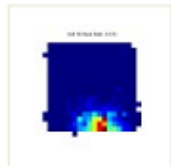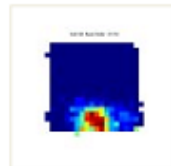
Supplementary Figure 5
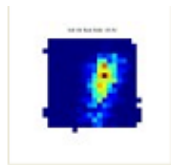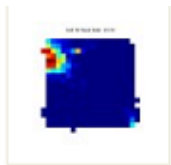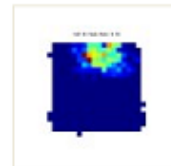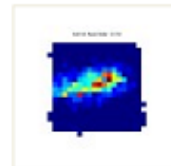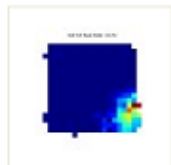
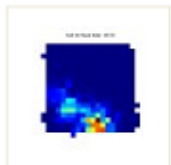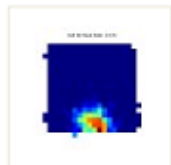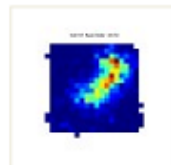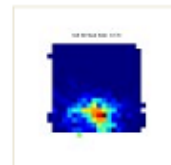CA1_49 CA1_50 CA1_51 CA1_52 CA1_53 CA1_54 CA1_55
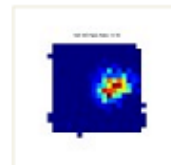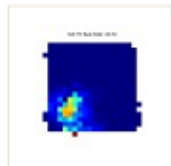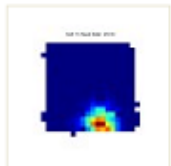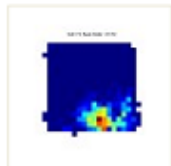
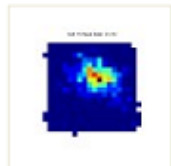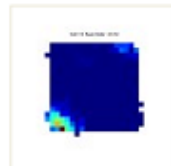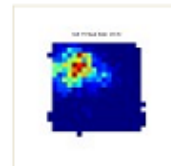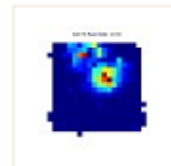CA1_56 CA1_57 CA1_58 CA1_59 CA1_60 CA1_61 CA1_62

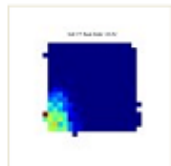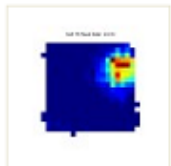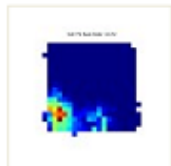CA1_63 CA1_64 CA1_65 CA1_66 CA1_67 CA1_68 CA1_69
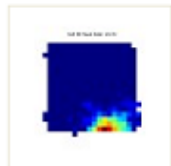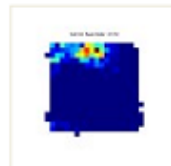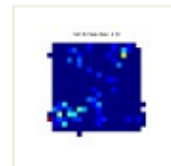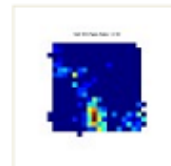
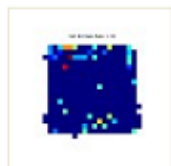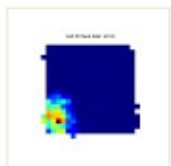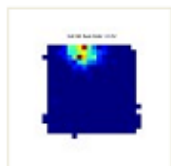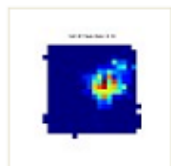CA1_70 CA1_71 CA1_72 CA1_73 CA1_74 CA1_75 CA1_76
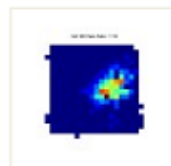
CA1_77 CA1_78 CA1_79 CA1_80 CA1_81 CA1_82 CA1_83

CA1_84 CA1_85 CA1_86 CA1_87 CA1_88 CA1_89 CA1_90
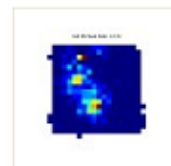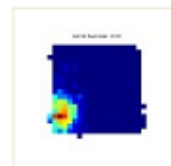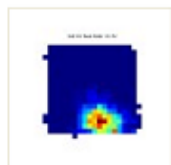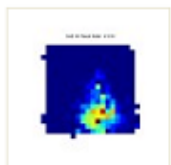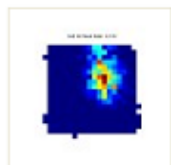
CA1_91 CA1_92 CA1_93 CA1_94 CA1_95 CA1_96 CA1_97
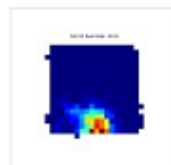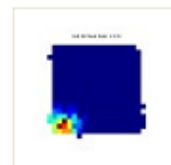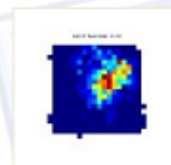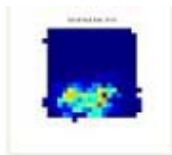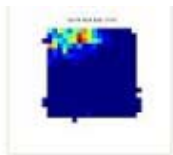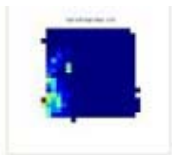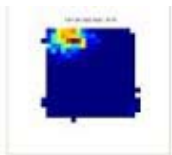
CA1_98 CA1_99 CA1_100 CA1_101 CA1_102 CA1_103 CA1_104
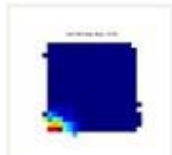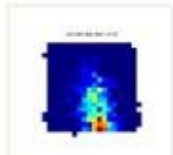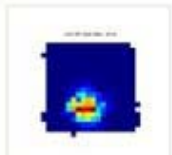
CA1_105 CA1_106 CA1_107 CA1_108 CA1_109 CA1_110 CA1_111
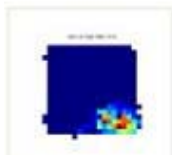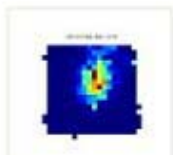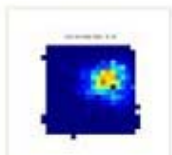
CA1_112 CA1_113 CA1_114 CA1_115 CA1_116 CA1_117 CA1_118
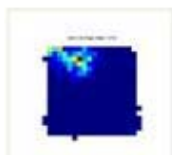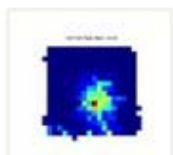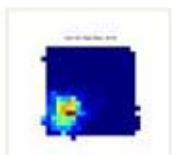
CA1_119 CA1_120 CA1_121 CA1_122 CA1_123 CA1_124 CA1_125
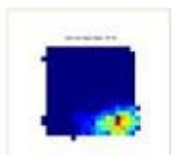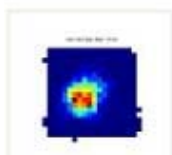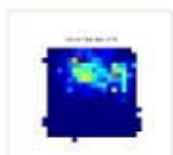
CA1_126 CA1_127 CA1_128 CA1_129 CA1_130 CA1_131 CA1_132
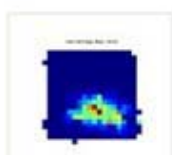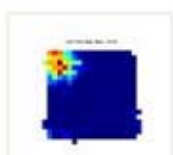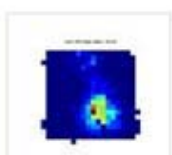
CA1_133 CA1_134 CA1_135 CA1_136 CA1_137 CA1_138 CA1_139
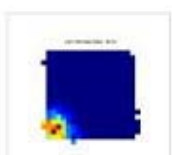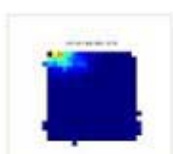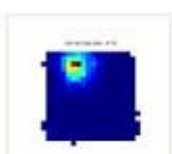
CA1_140 CA1_141 CA1_142 CA1_143 CA1_144 CA1_145 CA1_146
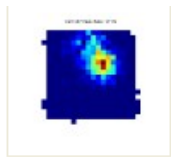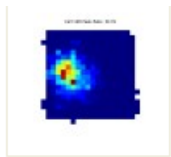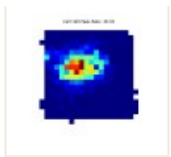
CA1_147	CA1_148	CA1_149	CA1_150	CA1_151	CA1_152	CA1_153
CA1_154	CA1_155	CA1_156	CA1_157	CA1_158	CA1_159	CA1_160
CA1_161	CA1_162	CA1_163	CA1_164	CA1_165	CA1_166	CA1_167
CA1_168	CA1_169	CA1_170	CA1_171	CA1_172	CA1_173	CA1_174
CA1_175	CA1_176	CA1_177	CA1_178	CA1_179	CA1_180	CA1_181
CA1_182	CA1_183	CA1_184	CA1_185	CA1_186	CA1_187	CA1_188
CA1_189	CA1_190	CA1_191	CA1_192	CA1_193	CA1_194	CA1_195
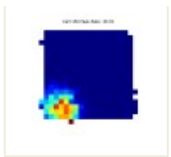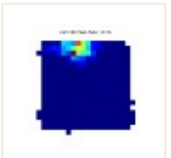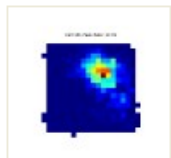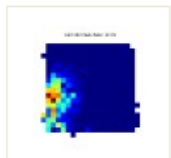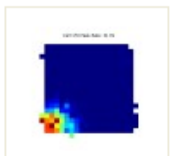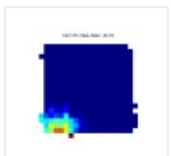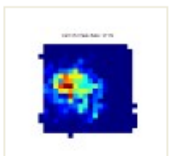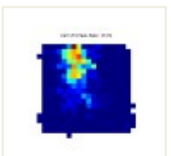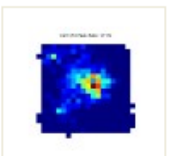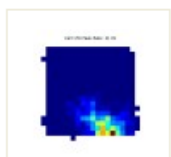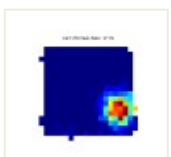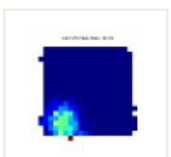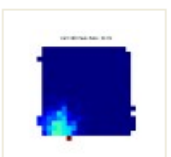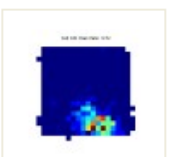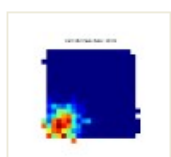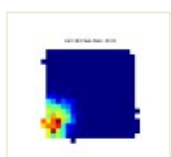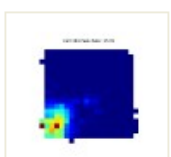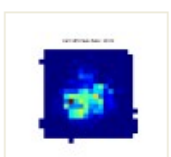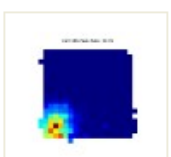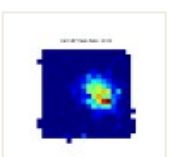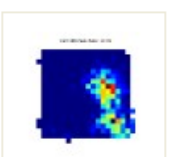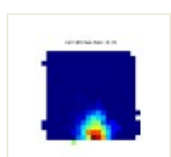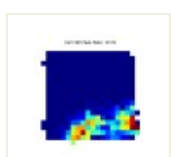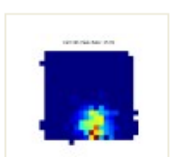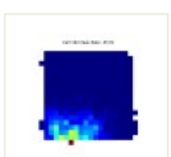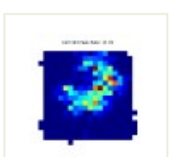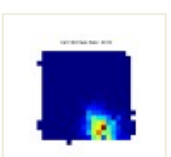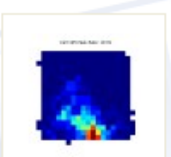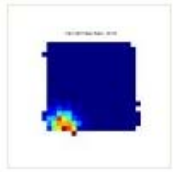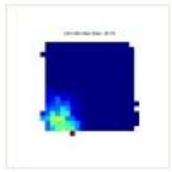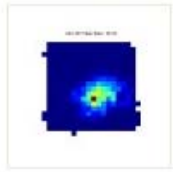
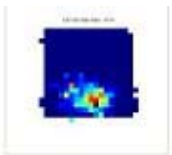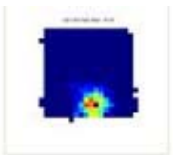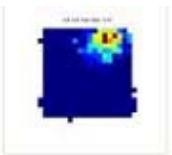CA1_245   CA1_246   CA1_247   CA1_248   CA1_249   CA1_250   CA1_251
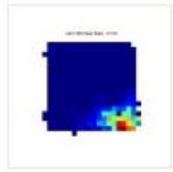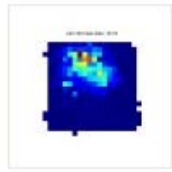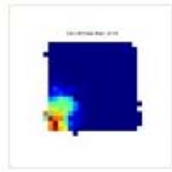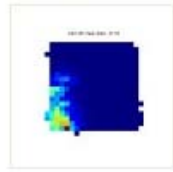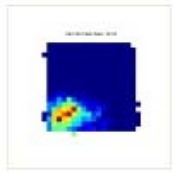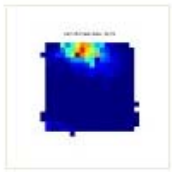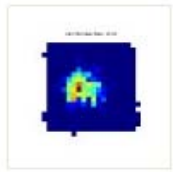
CA1_252   CA1_253   CA1_254   CA1_255   CA1_256   CA1_257   CA1_258
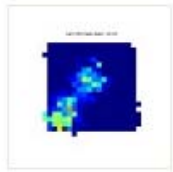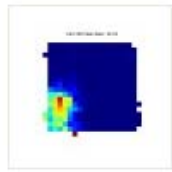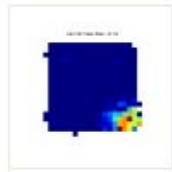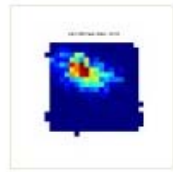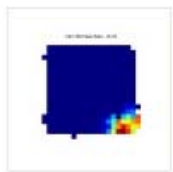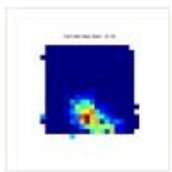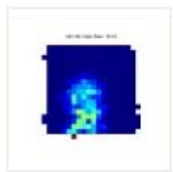
CA1_259   CA1_260   CA1_261   CA1_262   CA1_263   CA1_264   CA1_265
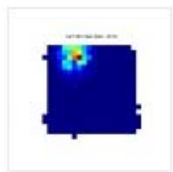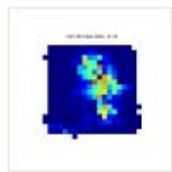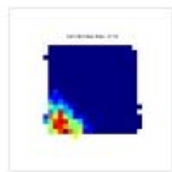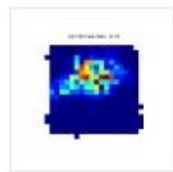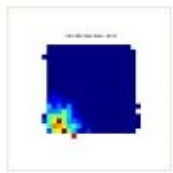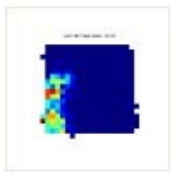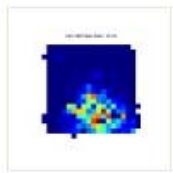
CA1_266   CA1_267   CA1_268   CA1_269   CA1_270   CA1_271   CA1_272
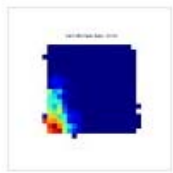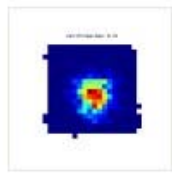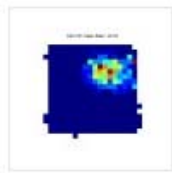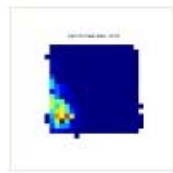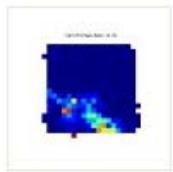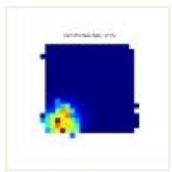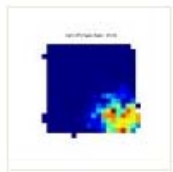
CA1_273   CA1_274   CA1_275   CA1_276   CA1_277   CA1_278   CA1_279
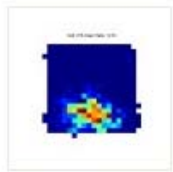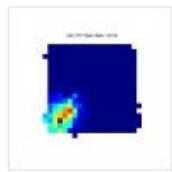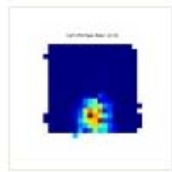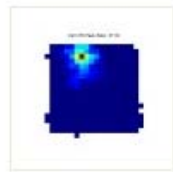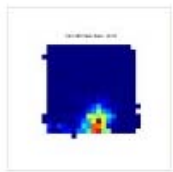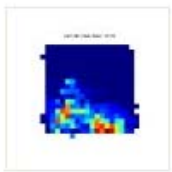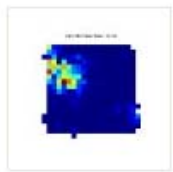
CA1_280   CA1_281   CA1_282   CA1_283   CA1_284   CA1_285   CA1_286
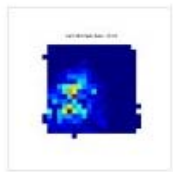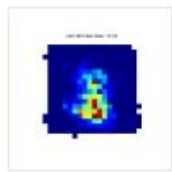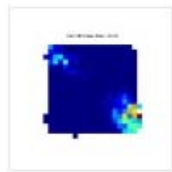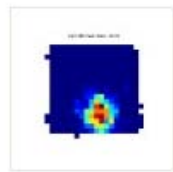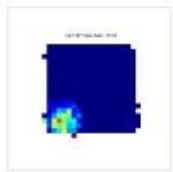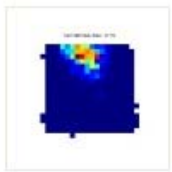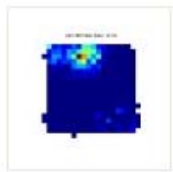
CA1_287   CA1_288   CA1_289   CA1_290   CA1_291   CA1_292   CA1_293
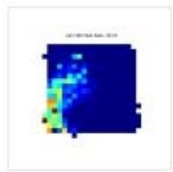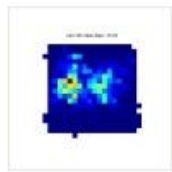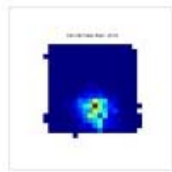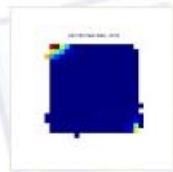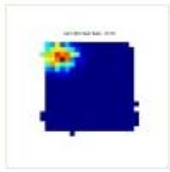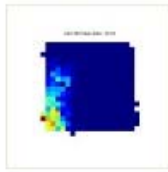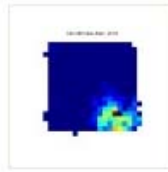
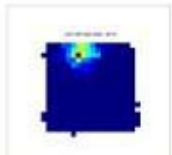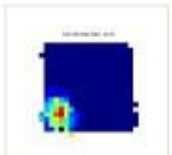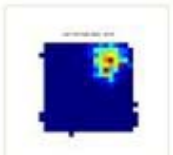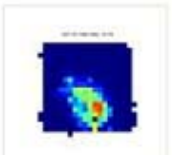CA1_294 CA1_295 CA1_296 CA1_297 CA1_298 CA1_299 CA1_300
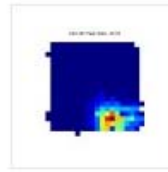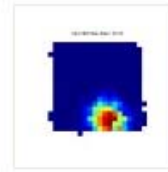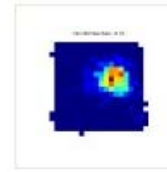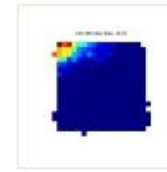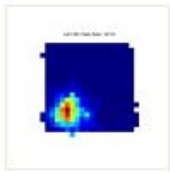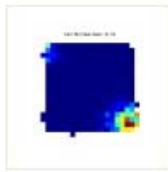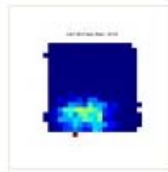
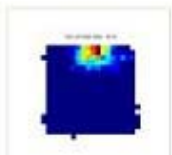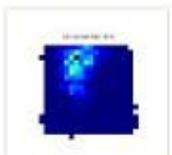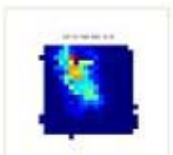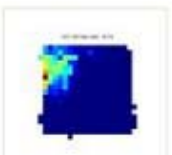CA1_301 CA1_302 CA1_303 CA1_304 CA1_305 CA1_306 CA1_307
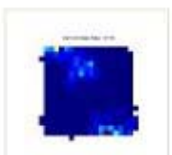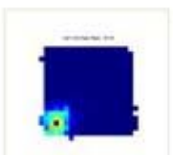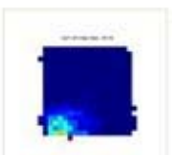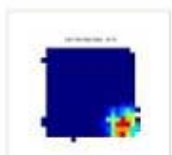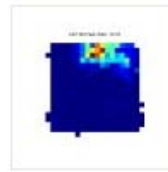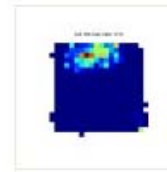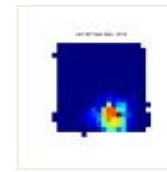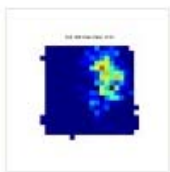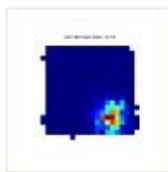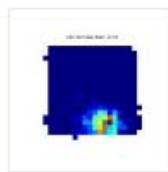
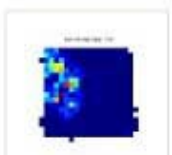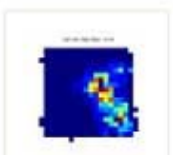CA1_308 CA1_309 CA1_310 CA1_311 CA1_312 CA1_313 CA1_314
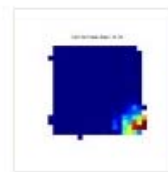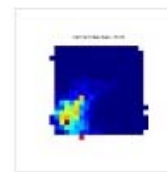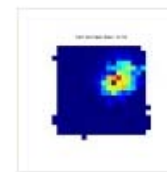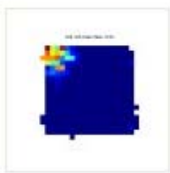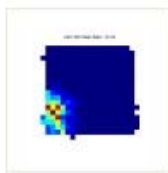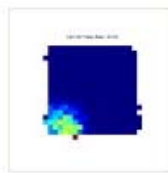
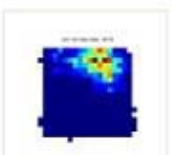CA1_315 CA1_316 CA1_317 CA1_318 CA1_319 CA1_320 CA1_321
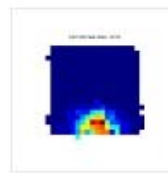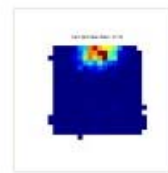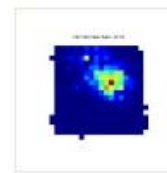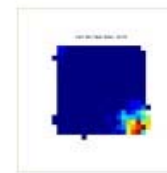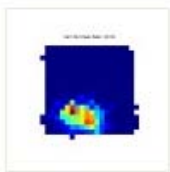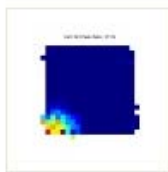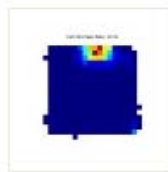
CA1_322 CA1_323 CA1_324 CA1_325 CA1_326 CA1_327 CA1_328
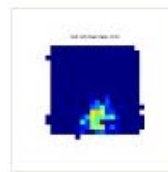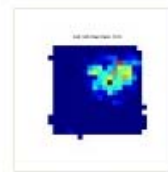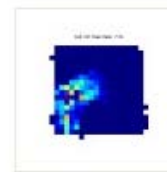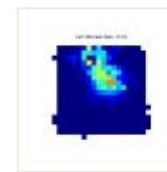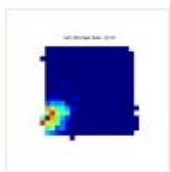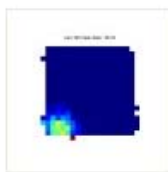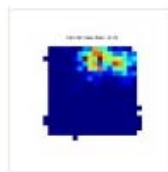
CA1_329 CA1_330 CA1_331 CA1_332 CA1_333 CA1_334 CA1_335
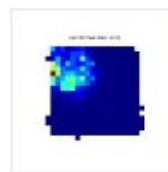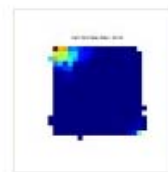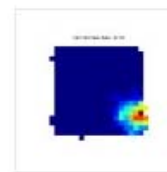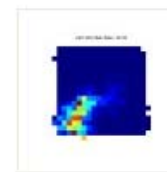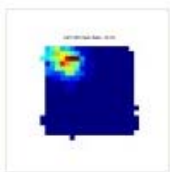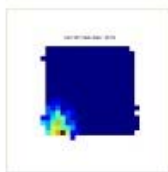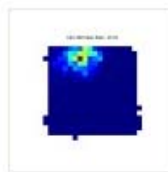
CA1_336 CA1_337 CA1_338 CA1_339 CA1_340 CA1_341 CA1_342
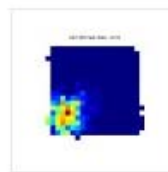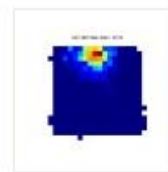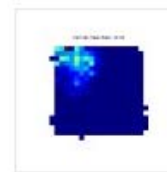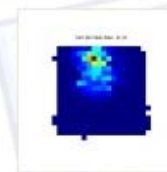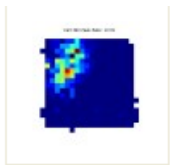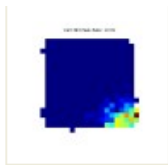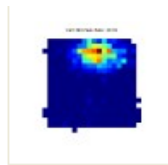
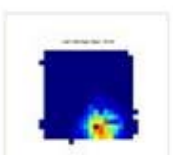CA1_392   CA1_393   CA1_394   CA1_395   CA1_396   CA1_397   CA1_398
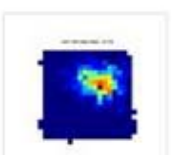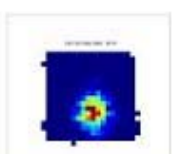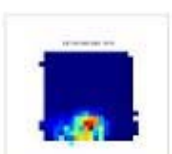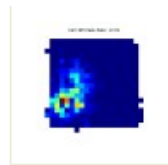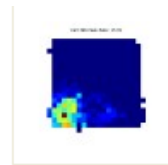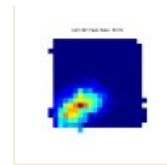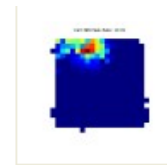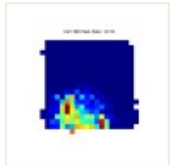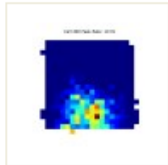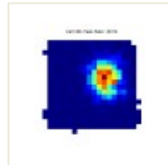
CA1_399   CA1_400   CA1_401   CA1_402   CA1_403   CA1_404   CA1_405
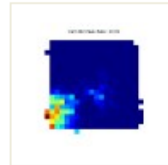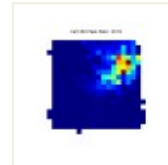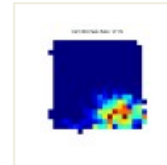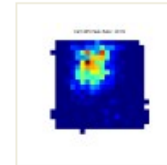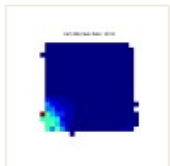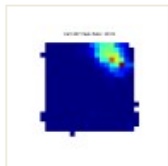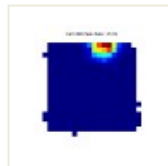
CA1_406   CA1_407   CA1_408   CA1_409   CA1_410   CA1_411   CA1_412
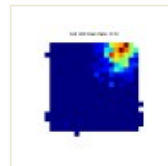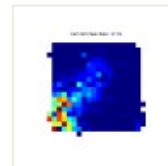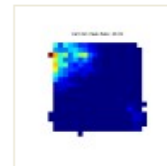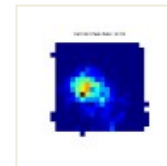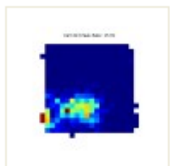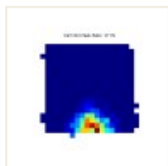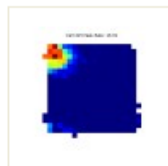
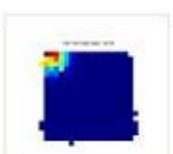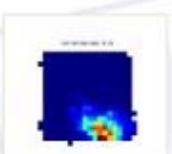CA1_413   CA1_414   CA1_415   CA1_416   CA1_417   CA1_418   CA1_419
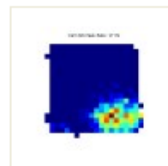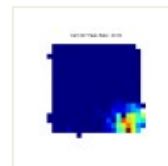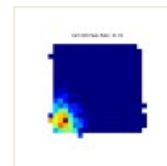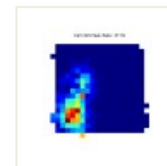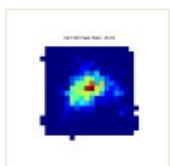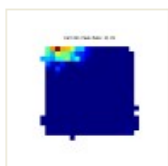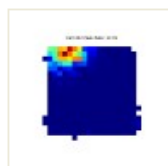
CA1_420   CA1_421   CA1_422   CA1_423   CA1_424   CA1_425   CA1_426

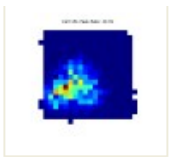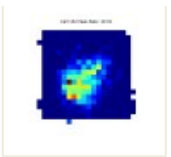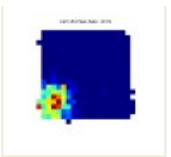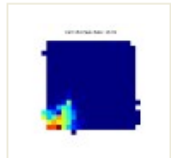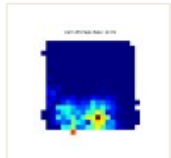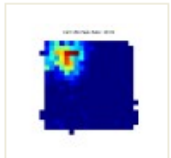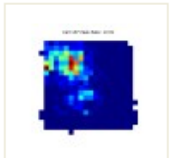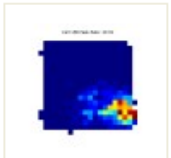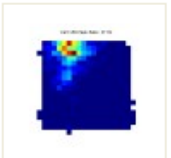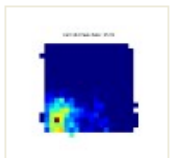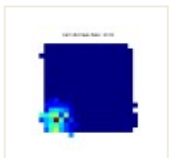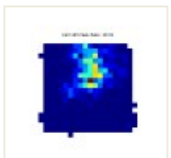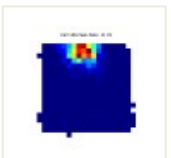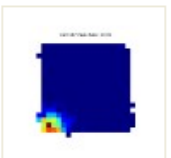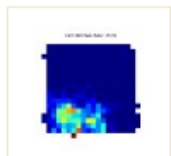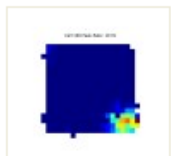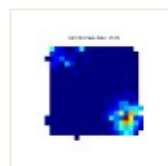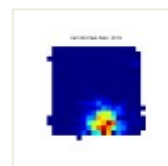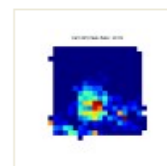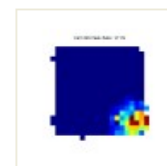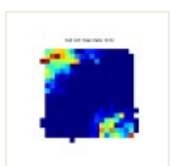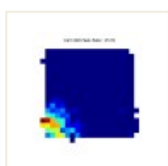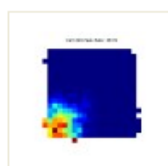CA1_427   CA1_428   CA1_429   CA1_430   CA1_431   CA1_432   CA1_433
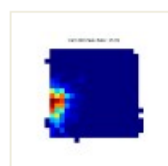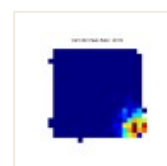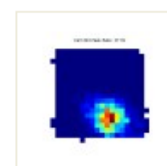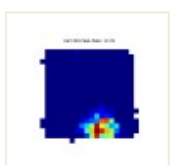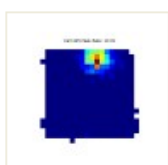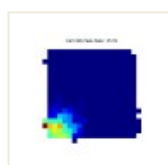
CA1_434   CA1_435   CA1_436   CA1_437   CA1_438   CA1_439   CA1_440
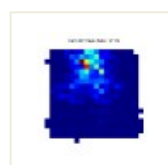
CA1_441	CA1_442	CA1_443	CA1_444	CA1_445	CA1_446	CA1_447
CA1_448	CA1_449	CA1_450	CA1_451	CA1_452	CA1_453	CA1_454
CA1_455	CA1_456	CA1_457	CA1_458	CA1_459	CA1_460	CA1_461
CA1_462	CA1_463	CA1_464	CA1_465	CA1_466	CA1_467	CA1_468
CA1_469	CA1_470	CA1_471	CA1_472	CA1_473	CA1_474	CA1_475
CA1_476	CA1_477	CA1_478	CA1_479	CA1_480	CA1_481	CA1_482
CA1_483	CA1_484	CA1_485	CA1_486	CA1_487	CA1_488	CA1_489
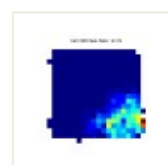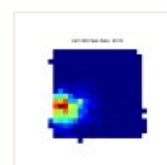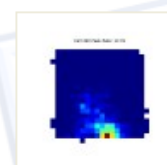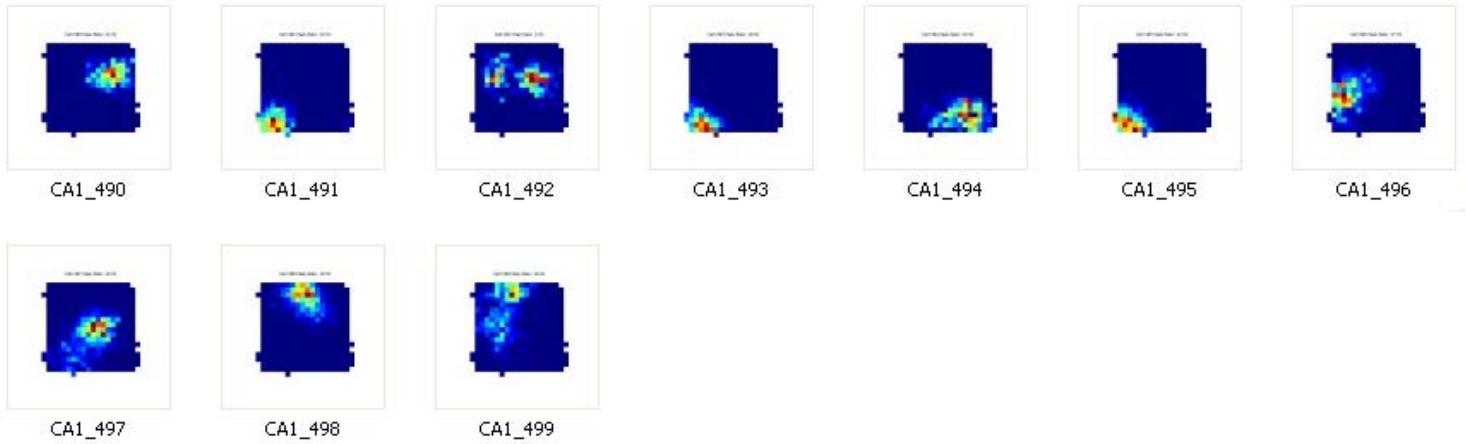
Supplementary Figure 5. Firing rate maps of all the "place cells" simulated as in Simulation 1 (see Suppl. Fig. 4) but with a different range of input grid spacing (70-93 cm instead of Simulation 1's 30-53 cm). The resulting fields are larger, with fewer subfields, and with more irregular shape than those in Suppl. Fig. 4. We also ran a simulation with an intermediate range of grid spacing (50-73 cm). As expected, the resulting place fields were intermediate in size and shape (data not shown).

Supplementary Figure 6
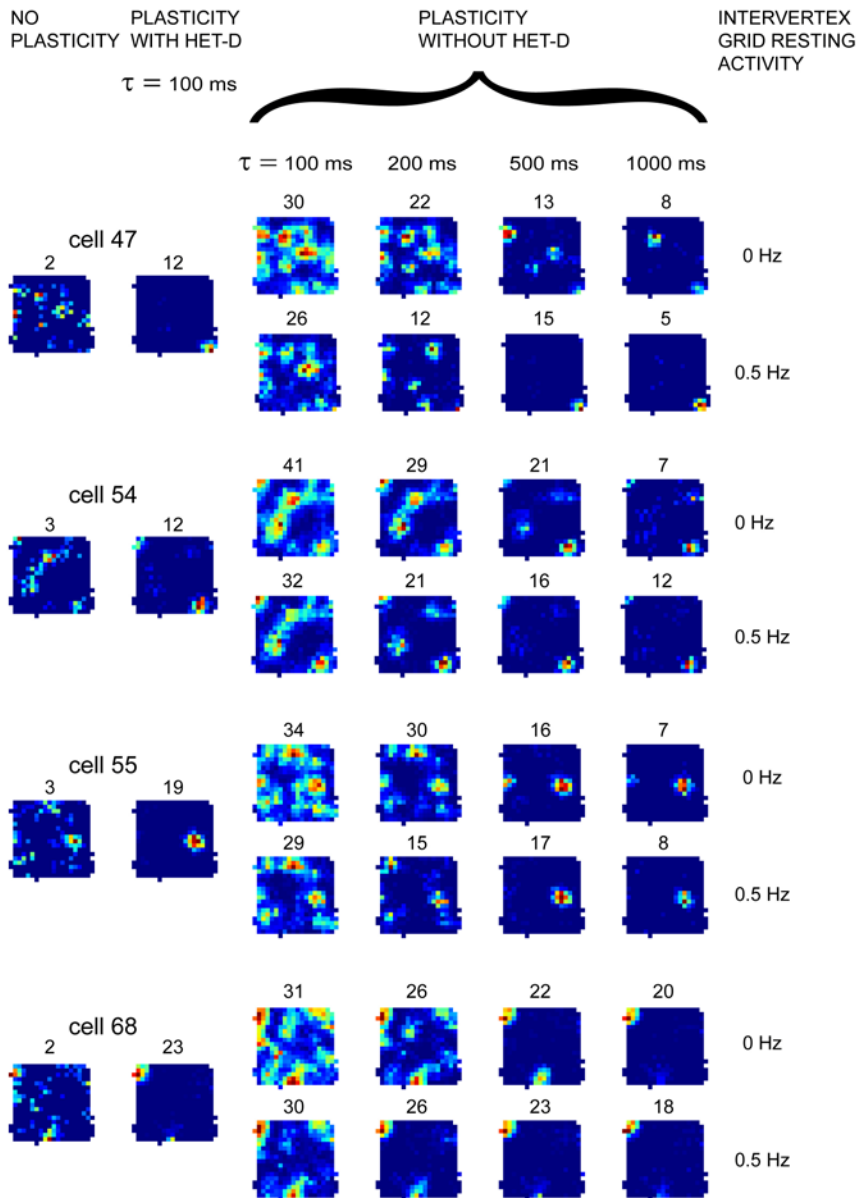
Supplementary Figure 6. Physiological alternatives to heterosynaptic depression. (A) Example of input grid cell with (right) and without (left) intervertex background activity. (B) Comparison

of rate maps of cells across different simulations. Rate maps in the first column were obtained from the simulation without synaptic plasticity. Rate maps in the second column were generated by the simulation with synaptic plasticity with heterosynaptic depression. Rate maps in the third to sixth columns were obtained from simulations with synaptic plasticity in which heterosynaptic depression was excluded, with increasing time constants (τ) used for the calculation of the presynaptic firing rate in the synaptic rule. The top and bottom rows of each pair show results for simulations in the absence or presence, respectively, of intervertex background activity in the grid inputs. Slower integration of presynaptic spikes compensates greatly for the lack of heterosynaptic depression, whereas the presence of intervertex grid background activity has a weaker contribution.

Results for Supplementary Figure 6. Recent experimental results at perforant path synapses suggest that presynaptic activity that is not directly controlled in *in vivo* experiments could disguise homosynaptic depression as heterosynaptic (Abraham et al., 2007). That is, the low-rate, spontaneous activity that typically occurs *in vivo* might provide a background level of activity of presynaptic cells that allows depression of these low-rate synapses using homosynaptic mechanisms (Abraham et al., 2007). A nonzero level of baseline activity in grid cells would cause the cells to fire at a low rate when the animal occupied a location in between the vertices of the grid. A longer time constant in the calculation of the momentary presynaptic firing rate would also provide a trace of presynaptic activity as the animal exits a vertex and enters an intervertex region. To test the interaction of these two possible mechanisms, we ran simulations in which the rule lacking heterosynaptic depression was used, with different time scales for the presynaptic firing rate decay, with or without spontaneous activity of grid cells in the intervertex spaces. For these simulations, we increased the value of θ_d compared to the other simulation of heterosynaptic depression in the main text (Fig. 2D and 2E). The threshold θ_d used in those simulations (0.05 Hz) was very low because it was important to demonstrate that even a minimal relaxation of the heterosynaptic property caused the failure of robust place-field formation in the model. Here we are in a logically opposite position, since we would like to test if the putative mechanisms can compensate for the lack of heterosynaptic depression, and so a higher threshold ($\theta_d = 0.3$ Hz) was chosen. This value approaches the rate of stimulation at which it becomes possible to induce homosynaptic depression in *in vitro* protocols (Steele and Mauk, 1999; Dudek and Bear, 1992; Mulkey and Malenka, 1992). The value of θ_p was the same as in Simulation 3 described in the main text ($\theta_p = 5$ Hz, see Fig. 2 and Table 1), in which the lack of heterosynaptic depression had its most dramatic effect. We tried time constants for the ongoing calculation of the presynaptic firing rate in the range 100–1000 ms. When included, intervertex activity was implemented by keeping the firing-rate of the grid cell above 0.5 Hz at every location in the environment (Supplementary Fig. 6A). Column 1 of Supplementary Figure 6B shows the rate map for each example cell produced with no plasticity; column 2 shows the rate map produced by Eq. (2) (i.e., including heterosynaptic plasticity); and columns 3-6 show the rate maps produced without heterosynaptic plasticity ($\theta_d = 0.3$ Hz) at 4 different time constants. For each cell, the first row of these 4 columns shows the rate maps produced with no spontaneous activity in between vertices and the second row shows the rate maps produced with an intervertex spontaneous activity of 0.5 Hz. Increasing the time constant of the presynaptic firing-rate decay improved the quality of place cells, moving from no spatial specificity due to the widespread runaway potentiation discussed in the previous section (τ = 100 ms) to a behavior that is comparable to the use of the intact rule of Eq. (2) (τ = 500-1000 ms). The addition of intervertex spontaneous activity was less effective. However, intervertex activity did provide a

positive contribution in combination with longer time constants, as relatively shorter time constants with intervertex activity performed comparably to longer ones without intervertex activity.

Supplementary Reference List

1. **Abraham WC, Logan B, Wolff A and Benuskova L**. "Heterosynaptic" LTD in the dentate gyrus of anesthetized rat requires homosynaptic activity. *J Neurophysiol* 98: 1048-1051, 2007.

2. **Dudek SM and Bear MF**. Homosynaptic long-term depression in area CA1 of hippocampus and effects of N-methyl-D-aspartate receptor blockade. *Proc Natl Acad Sci U S A* 89: 4363-4367, 1992.

3. **Mulkey RM and Malenka RC**. Mechanisms underlying induction of homosynaptic long-term depression in area CA1 of the hippocampus. *Neuron* 9: 967-975, 1992.

4. **Skaggs WE, McNaughton BL, Wilson MA and Barnes CA**. Theta phase precession in hippocampal neuronal populations and the compression of temporal sequences. *Hippocampus* 6: 149-172, 1996.

5. **Steele PM and Mauk MD**. Inhibitory control of LTP and LTD: stability of synapse strength. *J Neurophysiol* 81: 1559-1566, 1999.